Transportation Planning and Technology

ISSN: 0308-1060 (Print) 1029-0354 (Online) Journal homepage: www.tandfonline.com/journals/gtpt20

Preserving equity: multi-objective connected and automated vehicle (CAV) lane deployment in mixed traffic

Yu Lin, Bo Zou & Mohamadhossein Noruzoliaee

To cite this article: Yu Lin, Bo Zou & Mohamadhossein Noruzoliaee (25 Apr 2025): Preserving equity: multi-objective connected and automated vehicle (CAV) lane deployment in mixed traffic, Transportation Planning and Technology, DOI: 10.1080/03081060.2025.2495696

To link to this article: https://doi.org/10.1080/03081060.2025.2495696 https://doi.org/10.1080/03081060.2025.2495696

Preserving equity: multi-objective connected and automated vehicle (CAV) lane deployment in mixed traffic

Yu Lin[a], Bo Zou[b] and Mohamadhossein Noruzoliaee[c]

[a]Hangzhou International Innovation Institute, Beihang University, Beijing, People's Republic of China; [b]Department of Civil, Materials, and Environmental Engineering, University of Illinois Chicago, Chicago, IL, USA; [c]Department of Civil Engineering, University of Texas Rio Grande Valley, Edinburg, TX, USA

ABSTRACT

This paper investigates deploying connected and automated vehicle (CAV) lanes in transportation networks with a focus on measuring and preserving equity among travelers. A new metric is proposed to characterize equity based on (1) generalized travel cost per unit origin-destination (OD) distance for travelers on each OD pair and using each vehicle type and (2) maximum deviation of the standardized unit generalized travel cost from system average. A bi-level bi-objective program is developed to simultaneously minimize system travel cost and inequity while deploying CAV lanes. A solution algorithm that combines non-dominated sorting genetic algorithm II and variable neighborhood search is designed. Through extensive numerical experiments, we find (1) inequity is more prominent when travel demand is high; (2) human-driven vehicle travelers become more disadvantageous with lower CAV price and higher CAV automation; and (3) subsidy is effective in mitigating inequity, but a fee for using CAV lanes is less promising.

ARTICLE HISTORY
Received 25 June 2024
Accepted 15 April 2025

KEYWORDS
Equity; dedicated CAV lane deployment; bi-level bi-objective program; NSGA-II-VNS; pareto frontier; subsidy

Nomenclature

Sets

$\mathcal{N}$	set of nodes
$\mathcal{A}$	set of links
$\bar{\mathcal{A}}$	set of links with no candidate connected and automated vehicle (CAV) lanes
$\hat{\mathcal{A}}$	set of links with one or more candidate CAV lanes
W	set of origin-destination (OD) pairs
M	set of vehicle types
R_w^m	set of paths for vehicle type m. of OD pair w
I_a	set of lanes on link $a \in \hat{\mathcal{A}}$

Parameters

Λ_a	capacity of link a
$\bar{\mathbb{C}}$	capacity of a single human-driven vehicle (HV) lane
$\hat{\mathbb{C}}$	capacity of a single CAV lane

CONTACT Bo Zou bzou@uic.edu Department of Civil, Materials, and Environmental Engineering, University of Illinois Chicago, 2073 ERF, 842 W Taylor St., Chicago, IL 60607, USA

Y_a number of lanes on a physical link $a \in \hat{\mathcal{A}}$
VC_m variable operating cost of vehicle type m. per kilometer
η_m value of time (VOT) of travelers using vehicle type m
ρ_m price of vehicle type m
D_m^w travel demand using vehicle type m for OD pair w
D^w total travel demand for OD pair w
l_a length of link a

Variables

y_a^i Binary variable, equal to 1 if lane i on link $a \in \hat{\mathcal{A}}$ is converted to a CAV lane, and 0 otherwise
μ_m^w ratio of travel cost per unit OD distance of OD pair w to the system average, for vehicle type m
$f_{w,m}^r$ traffic flow on path r of OD pair w for vehicle type m
t_a^m travel time of vehicle type m on link a
$c_{w,m}^r$ generalized travel cost of travelers using vehicle type m on path r of OD pair w
C_w^m minimum generalized travel cost by vehicle type m for OD pair w
v_a vehicle flow on link a
v_a^m vehicle flow of type m on link a

1. Introduction

Connected and autonomous vehicles (CAV) have been gaining significant momentum with many anticipated benefits to the transportation system, including increased road capacity (Chen et al. 2017; Lu et al. 2020; Talebpour and Mahmassani 2016), improved traffic operations (Gong, Shen, and Du 2016; Levin and Boyles 2016; Li, Elefteriadou, and Ranka 2014; van den Berg and Verhoef 2016), reduced vehicle energy use (Han, Ma, and Zhang 2020; Vahidi and Sciarretta 2018), and enhanced traffic safety (Kalra and Paddock 2016; Liu and Khattak 2016). However, as the transition from human-driven vehicles (HVs) to CAVs will be a gradual process, HVs and CAVs are expected to coexist on roads in the foreseeable future. Because of this, determining the optimal planning of CAV infrastructure within existing road networks in a mixed CAV-HV environment is an area of both research and practical interest.

In CAV infrastructure planning research, the idea of deploying dedicated CAV lanes – through the conversion of some HV lanes to lanes only used by CAVs – to accommodate CAV traffic while allowing mixed CAV-HV traffic to use the remaining lanes in a road network has garnered special interest (e.g. Chen et al. 2016; Kumar, Guhathakurta, and Venkatachalam 2020; Liu and Song 2019). The existing research focused mainly on improving system efficiency and promoting CAV adoption. However, little attention has been paid to equity, despite its importance in CAV lane deployment. By converting some HV lanes to dedicated CAV lanes, travelers using CAVs are expected to save trip times due to the allocation of dedicated road space and increased capacity of those lanes thanks to CAV technologies (e.g. vehicle-to-vehicle communications). But for travelers using HVs, the loss of road space may result in increased trip times. Thus, in determining what lanes to convert for dedicated CAV use, it is desired and important to preserve equity between CAV and HV travelers, in addition to maximizing system efficiency. To this end, this study formulates a bi-level bi-objective mathematical program. By solving the program using a customized algorithm, extensive numerical experiments are conducted to generate insights and policy implications.

Overall, this study aims to make four contributions. First, we propose a new metric to characterize system equity while deploying CAV lanes. The equity metric measures the maximum deviation of the generalized travel cost per unit origin-destination (OD) distance from the system average, for travelers of any OD pair and taking either vehicle type (CAV or HV). This metric is highly relevant as ideally, we desire all travelers to have the same unit generalized travel cost. To preserve equity, minimizing this maximum deviation is sought and considered the equity-side objective. Constructing the equity metric involves normalization of the unit generalized travel cost, which allows for equity comparison between different networks.

Second, we propose a bi-level bi-objective program to tackle the optimal CAV lane deployment. At the upper level, the program minimizes system travel cost and equity metric value simultaneously, by selecting and converting HV lanes to dedicated CAV lanes. The minimization anticipates responses of CAV and HV travelers, which are reflected in the distribution of traffic on the network and characterized as a multi-class user equilibrium at the lower level. To solve the equilibrium, an equivalent optimization model is presented. In doing so, a new link notation is adopted to accommodate the fact that converted CAV lanes can only be used by CAVs, while the remaining HV lanes can be used by both HVs and CAVs. To solve the overall bi-level bi-objective program, a customized algorithm that harnesses the complementary strengths of non-dominated sorting genetic algorithm II (NSGA-II) in global search and variable neighborhood search (VNS) in local search for solutions is proposed.

The next two contributions are related to insights and policy implications from implementation of the program. The third contribution mainly pertains to understanding the tradeoff between system efficiency and equity and its evolution with changes in key system parameters. It is found find that the tradeoff space varies by network and by where system travel cost and equity lie on the Pareto frontier. When travel demand is low and the network is relatively uncongested, inequity is not a significant concern. As demand increases, inequity starts to appear, first across different ODs and then between CAV and HV travelers. When CAV price or CAV traveler VOT is lowered, which is likely as CAVs continue to mature, the equity gap between CAV and HV travelers will be widened, suggesting a need for interventions.

Our fourth contribution pertains to such interventions. We explore the possibility of subsidizing HV travelers and levying a fee from CAV travelers for CAV lane use. Numerical results show that subsidizing HV travelers by an appropriate amount can improve equity as well as system travel cost. However, over-subsidy will widen the equity gap, as disadvantaged HV travelers become advantaged travelers. On the other hand, when travel demand is high and the network is congested, subsidy has limited effect on the Pareto frontier. Subsidy can push the Pareto frontier toward better equity and system travel cost when CAV price and CAV traveler VOT are reduced. In most cases, subsidy is also economically justifiable as the associated reduction in system travel cost exceeds the subsidy amount. Introducing a CAV lane use fee is not as promising as subsidizing HV travelers, as it not only increases CAV traveler cost but also offers a less clear improvement in equity.

The remainder of the paper is organized as follows. In Section 2, we review the relevant literature, based on which the gaps we aim to fill are identified. Section 3 provides a numerical characterization of the problem, including the network representation, the equity metric, and the bi-level bi-objective optimization program. Section 4 proposes a customized algorithm to solve the optimization program. Section 5 conducts numerical experiments on the Nguyen-Dupuis network and a south Florida network. Section 6 concludes and suggests directions for future research.

2. Literature review

This section conducts a review of the relevant literature, spanning three areas: CAV lane deployment, multiple-objective transportation network design, and equity considerations in transportation. Based on the literature review, we identify the research gaps to fill and highlight the importance of filling these gaps.

2.1. CAV lane deployment

We begin our literature review by first looking at the implications of CAVs for road capacity, which has drawn quite a bit of interest from researchers (Levin and Boyles 2016; Shladover 2018; van den Berg and Verhoef 2016). Chen et al. (2017) developed detailed analytical formulations for road capacity in mixed automated vehicle (AV)-HV traffic, taking into account (1) AV penetration rate, (2) micro/mesoscopic AV and HV characteristics, and (3) different lane policies to accommodate AVs. Chen et al. (2022) investigated the distribution of a single lane capacity with mixed AV-HV traffic flow, derived capacity bounds, and found that capacity can vary with AV penetration in and patterns of the traffic flow mix. Research attention has also been given to having CAVs travel on dedicated lanes. Tientrakool, Ho, and Maxemchuk (2011) showed that the capacity of a dedicated CAV lane can be nearly three times that of a conventional lane. Using simulations, Ye and Yamamoto (2018) investigated the effect of dedicated CAV lanes on highway capacity and examined the dynamic relationship among dedicated CAV lanes, and CAV automation and penetration levels. Razmi Rad et al. (2020) developed a conceptual framework to analyze different CAV lane design configurations and utilization policies on motorways.

From a network perspective, a thread of research has looked into transportation network equilibrium with mixed AV-HV traffic. Some of the works specifically pursued optimal AV lane deployment, mostly with the objective of improving system efficiency. Chen et al. (2016) proposed a bi-level model to determine the optimal AV lane deployment with decisions on timing, location, and quantity of AV lane deployment. Three plans: without AV lane, deploying all AV lanes at once, and dynamic implementation were examined. Chen, Wang, and Meng (2019) investigated the AV lane deployment problem considering AV price uncertainty and purchase subsidy. The authors proposed a purchase subsidy strategy to improve system performance in terms of total travel time and promote AV adoption. Liu and Song (2019) studied the AV/toll (AVT) lane problem, in which AVT lanes are freely accessible by AVs, while HVs need to pay a toll to access the AVT lanes. Wang et al. (2021) further studied the AVT lanes deployment problem with detailed toll design under elastic travel demand. More recently, Seilabi et al. (2023)

considered lane reallocation policy and market size uncertainty while deploying dedicated CAV lanes, with the objective of minimizing vehicle emissions.

2.2. Multiple-objective transportation network design

As both efficiency and equity are of interest while deploying CAV lanes, bi-objective optimization is more relevant. Such a problem falls into the general category of multi-objective network design problems (MNDP) (Chen et al. 2010; Lin and Xie 2011; Miandoabchi et al. 2013; Sharma and Mathew 2011; Sohn 2011; Ye and Wang 2018). In the MNDP literature, a subgroup of MNDP studies dealing with environmental objectives or social equity of particular relevance is especially worth noting. Wang and Szeto (2017) investigated multi-objective road network design which simultaneously optimizes system travel cost, emission cost, and noise excess cost using a chemical reaction optimization algorithm. Ferguson, Duthie, and Waller (2012) developed two bi-level optimization models to minimize system total travel time and system emissions respectively, to assess the trade-off between travel delay and emissions. The results showed that reducing traffic congestion does not necessarily lead to minimum emissions for some criteria pollutants. Chen and Xu (2012) employed a goal programming approach to road network design under demand uncertainty, in which a priority structure is specified to achieve the efficiency, environment, and equity objectives. A simulation-based genetic algorithm was developed to solve the goal programming models.

2.3. Equity considerations in transportation network design

Transportation network design changes capacity of the existing road network, which can cause redistribution of traffic and subsequently spatial inequity on the network. Spatial inequity in a transportation network, generally speaking, refers to travelers of different ODs not having access to the same quality of mobility. Various metrics were proposed to measure spatial inequity, such as based on GINI coefficient, Theil index, and the notion of accessibility (Ben-Elia and Benenson 2019; Feng and Zhang 2014; Shi 2021). Additionally, the ratio of travel cost before and after transportation network design was adopted as an equity constraint. Meng and Yang (2002) pointed out that performing transportation network design by minimizing total system cost may end up increasing travel cost for some OD pairs. The authors proposed an OD travel cost ratio before and after the road network design to characterize OD equity.

Besides spatial equity, Yang and Zhang (2002) investigated the problem of tolling network design considering social equity between poor and rich travelers who pay the same toll, along with spatial equity among travelers of different ODs. Szeto and Lo (2006) investigated time-dependent road network design by introducing inter-generational equity, and examined the tradeoff between societal and individual perspectives for the planning period. Santos, Antunes, and Miller (2008) introduced three equity criteria: accessibility to low-accessibility population centers, dispersion of accessibility values across population centers, and dispersion of accessibility across all population centers and across centers in the same region. These criteria were incorporated into a road network design model to maximize a weighted sum of accessibility and equity objectives. Sumalee, Shepherd, and May (2009) proposed a method to determine road user charging schemes by considering three objectives of social welfare, charging revenue, and distributional equity. NSGA-II-based solution methods were developed to solve the multi-objective design. Using John Rawls's theory of justice, Behbahani, Nazari, Partovifar et al. (2019) developed a bi-level integer program to investigate road network design. The authors found that compared to the classic method, John Rawls' approach increases accessibility of low-to-medium accessibility groups.

2.4. Gaps in the literature and importance of filling these gaps

Based on the review of the existing literature, very little research has looked into equity while deploying CAV lanes. We are aware of only two relevant works. One sought to jointly deploy AV lanes and determine road tolls, by minimizing a weighted sum of travel time, emission, and electricity consumption cost (Pourgholamali, Miralinaghi, and Ha 2023). Equity was considered through constraining exceeding HV travel cost and ensuring revenue neutrality. The other work focused on deploying a CAV platoonable corridor (Zhu et al. 2023), by minimizing a weighted sum of infrastructure upgrade cost, generalized travel cost, and inequity cost. The inequity cost was defined as the increase in generalized travel cost of HV travelers compared to without the CAV platoonable corridor. The inequity measure, as it is cost based, is network dependent: larger networks and more HV travelers are likely to show greater inequity costs. Thus, it would be difficult to use the measure to compare inequity between networks of different sizes.

In view of the above, three important gaps in the literature are identified. First, a network-independent equity metric that allows for inter-network equity comparison is needed in the context of CAV lane deployment. Second, the tradeoff space between system efficiency and equity while deploying CAV lanes, including how the tradeoff evolves with changes in key system parameters, has not been investigated nor well understood. Third, to mitigate inequity, the possibility of subsidizing HV travelers have not been explored. Our paper attempts to fill these gaps. Filling these gaps will advance our ability to understand and address the equity issue in CAV lane deployment. This in turn supports more informed infrastructure planning, investment, and policymaking as the society embraces connected and automated mobility.

3. Problem formulation

This section presents the mathematical formulation of our problem. We begin by introducing the network representation (Section 3.1). Then, the equity metric used in this study is proposed (Section 3.2). The bi-level bi-objective mathematical program for determining the optimal CAV lane deployment considering both system efficiency and equity is described in Section 3.3.

3.1. Network representation

We let $G(\mathcal{N}, \mathcal{A})$ represent the transportation network, where $\mathcal{N}$ denotes the set of nodes and $\mathcal{A}$ denotes the set of links connecting adjacent nodes. $\mathcal{A} = \bar{\mathcal{A}} \cup \hat{\mathcal{A}}$. $\bar{\mathcal{A}}$ denotes the set of links with no candidate CAV lane. $\hat{\mathcal{A}}$ denotes the set of links with one or more candidate CAV lanes. We further decompose $\hat{\mathcal{A}}$. into $\hat{\mathcal{A}}_1$ and $\hat{\mathcal{A}}_2$. $\hat{\mathcal{A}}_1$ denotes the set of virtual links each consisting of dedicated CAV lane(s) only. $\hat{\mathcal{A}}_2$ denotes the set of virtual links each consisting of HV lane(s) only. An HV lane can be used by both HVs and CAVs, while a dedicated CAV lane can only be used by CAVs. In other words, if a physical link $a \in \hat{\mathcal{A}}$ has both dedicated CAV and HV lanes, a is decomposed into two virtual links $a' \in \hat{\mathcal{A}}_1$. and $a'' \in \hat{\mathcal{A}}_2$. a' connects the same nodes as a, and consists of dedicated CAV lane(s) only. a'' also connects the same nodes as a, and consists of HV lane(s) only. If no lane on a is converter dedicated CAV use, then a only has a''. In this study, we always keep at least one HV lane for each physical link $a \in \hat{\mathcal{A}}$. Thus, it cannot happen that a only has a'. By decomposing $\hat{\mathcal{A}}$ into $\hat{\mathcal{A}}_1$ and $\hat{\mathcal{A}}_2$, $\mathcal{A} = \bar{\mathcal{A}} \cup \hat{\mathcal{A}}_1 \cup \hat{\mathcal{A}}_2$.

Let us use a simple network in Figure 1 to further illustrate this. Figure 1(a) presents the conventional link notation, where any two nodes are connected by at most one link with the direction indicated by the arrow. That link corresponds to a physical road link. In Figure 1(a), links 1, 4, 5, and 6 contain only HV lanes which cannot be converted to dedicated CAV lanes. These links belong to $\bar{\mathcal{A}}$. On the other hand, links 2, 3, 7, and 8 (in red) each have one or multiple lanes converted to dedicated CAV lanes, and also have at least one HV lane. These links belong to $\hat{\mathcal{A}}$. With $\mathcal{A} = \bar{\mathcal{A}} \cup \hat{\mathcal{A}}_1 \cup \hat{\mathcal{A}}_2$, link 2 is replaced by two virtual links: $2'$ from $\hat{\mathcal{A}}_1$ and $2''$ from $\hat{\mathcal{A}}_2$. Similarly for links 3, 7, and 8. This is shown in Figure 1(b).

With the above link notations, the sets of feasible paths for CAVs and HVs for a given OD pair can be different. As an example, for OD pair 1-2, the feasible paths for HVs are comprised of: link 1, link 3''→link 4, and link 2''→link 6→link 4. These paths are also feasible for CAVs of the same OD pair. However, the set of feasible paths for CAVs further contains: link 3'→link 4, and link 2'→link 6→link 4.

3.2. The equity metric

Equity is an ever-present issue in human society. According to the Merriam-Webster Dictionary (2024), equity is about the fairness or justice in the way people are treated. Equity can be interpreted from different perspectives, such as utilitarianism,

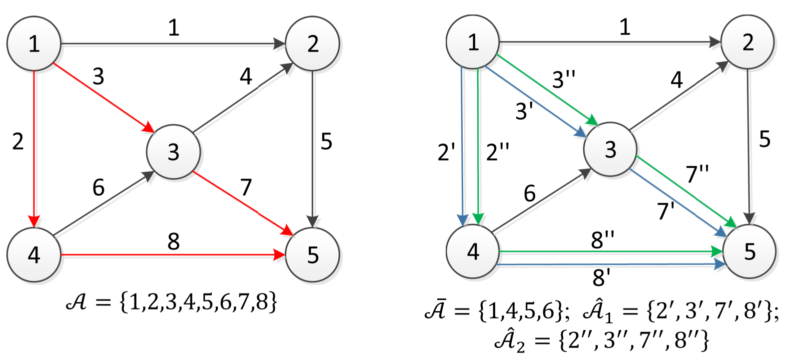

Figure 1. Illustration of (a) conventional road network representation comprised of physical links with (in red) and without (in black) dedicated CAV lane(s) on the links, and (b) proposed network representation where $\mathcal{A} = \bar{\mathcal{A}}$ (set of physical links with no CAV lanes, in black) $\cup\ \hat{\mathcal{A}}_1$(set of CAV *virtual links*, in green)$\cup\hat{\mathcal{A}}_2$(set of HV virtual links, in blue).

libertarianism, and Rawls' egalitarianism. The concept of equity has been extensively discussed in many studies (Dworkin 2018). For instance, Sawyer et al. defined fairness as 'equal treatment for equal individuals while reserving preferential treatment for those who deserve it.' Many measures have been proposed (Atkinson index, Gini coefficient, and Theil index, to name a few); they all point to the essence of equity that is to achieve a reasonable distribution of resources (Behbahani, Nazari, Jafari Kang et al. 2019; Pereira, Schwanen, and Banister 2017). In the transportation domain, equity generally involves two categories: horizontal equity and vertical equity (Litman 2002; 2020). Horizontal equity refers to the principle that individuals or groups in similar situations/conditions should be treated equally. Vertical equity rests on the idea that individuals or groups in different situations/conditions should receive different treatments, in order to reduce inequality.

In transportation network design, changes in infrastructure provision can cause redistribution of trips on the network, which may improve or worsen equity. To analyze the impact of road network design on equity, concepts such as social equity, spatial equity, and user equity have been proposed (Meng and Yang (2002); Yang and Zhang (2002) Szeto and Lo (2006)). Despite differences in terminology, the analytical frameworks of these studies generally align with two dimensions: horizontal equity and vertical equity. Specifically for CAV lane deployment with a mix of HV and CAV traffic, horizontal equity seeks to achieve equal travel cost per unit distance, among travelers of different OD pairs using the same vehicle type. For vertical equity, the equity concern is to reduce the difference in travel cost per unit distance between travelers using different vehicle types. In this study, we propose an equity metric that accounts for both horizontal and vertical equity. The metric builds on μ values which characterize the travel cost per unit distance for each OD pair and each vehicle type, relative to the average of the travel costs per unit distance over all OD pairs and both vehicle types. Our equity is defined as the maximum deviation of any μ value from the mean μ value, which can be viewed as an L_p distance measure with the norm $p \to \infty$ (Olivier, Lodi, and Pesant 2022). The equity objective is to minimize this maximum deviation. The idea of performing min–max derives from Rawls' principle of justice (Rawls 1971) and has been used for equity measurement in many contexts such as facility location (Marsh and Schilling 1994; Ogryczak 2000), truck driver scheduling (Hamdan et al. 2024), machine scheduling (Qu 2018), and air traffic management (Guo et al. 2022; Zografos and Jiang 2019). For the sake of clarity, we draw Figure 2 to present the derivation process of equity metric. Below we detail the equity metric development.

A few notations need to be introduced for the metric development. For a traveler, the generalized travel cost incurred by using vehicle type $m \in \{\text{HV}, \text{CAV}\}$ of OD pair w is denoted by C_m^w and calculated later in Section 3.3.2. The OD distance for OD pair w, denoted by $l_{\min}^w$, is the length of the shortest-distance path connecting the OD pair. The generalized travel cost per unit OD distance for HV travelers and CAV travelers of OD pair w are thus $C_{\text{HV}}^w / l_{\min}^w$ and $C_{\text{CAV}}^w / l_{\min}^w$. For the transportation system as a whole, the total generalized travel cost incurred by all travelers across the network is $\sum_m \sum_a c_a^m v_a^m$, where c_a^m is the generalized travel cost on link $a \in \bar{\mathcal{A}} \cup \hat{\mathcal{A}}_1 \cup \hat{\mathcal{A}}_2$ of travelers using vehicle type m. v_a^m is traffic flow of vehicle type m on link a. The derivation of c_a^m

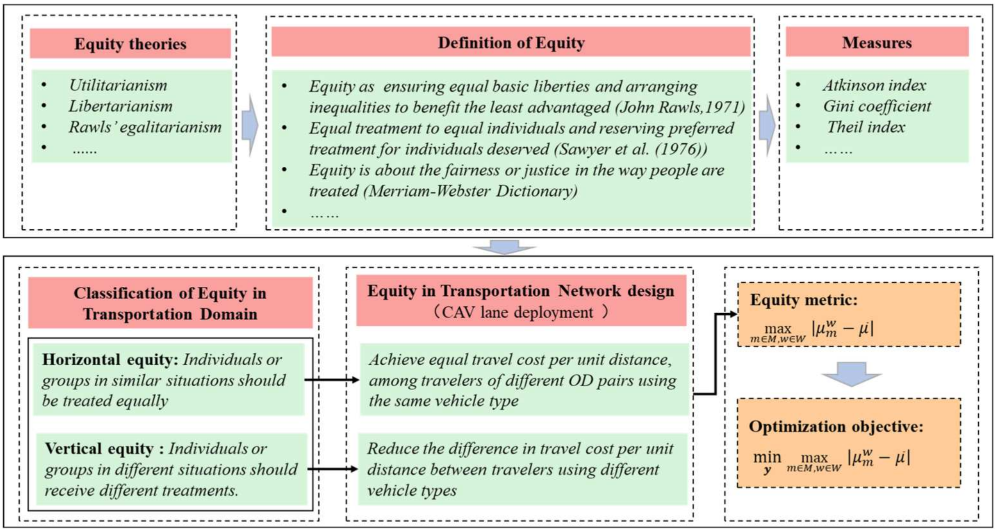

Figure 2. The derivation process of equity metric.

and v_a^m is deferred to Section 3.3.2. Note that in line with the link notation in Section 3.1, the summation of a is over physical links in $\bar{\mathcal{A}}$ as well as virtual links in $\hat{\mathcal{A}}_1$ and $\hat{\mathcal{A}}_2$.

With the above notations, we express the average generalized travel cost per unit OD distance for all travelers on the network:

$$U = \frac{\sum_m \sum_a c_a^m v_a^m}{\sum_w D^w l_{\min}^w} \tag{1}$$

where D^w is travel demand of OD pair w, i.e. $D^w = D_{\mathrm{HV}}^w + D_{\mathrm{CAV}}^w$.

For a traveler of OD pair w, the ratio of the generalized travel cost per unit OD distance incurred by the traveler to the average generalized travel cost per unit OD distance is expressed in (2)-(3), for HV and CAV travelers respectively.

$$\mu_{\mathrm{HV}}^w = \frac{C_{\mathrm{HV}}^w}{l_{\min}^w U} \quad \forall\, w \in W \tag{2}$$

$$\mu_{\mathrm{CAV}}^w = \frac{C_{\mathrm{CAV}}^w}{l_{\min}^w U} \quad \forall\, w \in W \tag{3}$$

In (2)–(3), we take the ratio to 'normalize' the generalized travel cost per unit OD distance. Doing so facilitates comparison between networks of different sizes and characteristics. For example, a network composed primarily of highways will likely have a much higher generalized travel cost per unit OD distance than another network composed mainly of local roads and streets. In this case, comparing the unit generalized travel cost between the two networks would not be very sensible. Through normalization, the μ values of different networks become more comparable, as each μ is about the *relativity* of the unit generalized travel cost for an OD and a vehicle type with respect to the average of the network.

The system average ratio $\bar{\mu}$ is obtained by taking the weighted average of μ_m^w's over all OD pairs and across both HV and CAV travelers, weighted by the respective travel demands, as shown in (4). The maximum deviation of any ratio μ_m^w from the system average ratio, expressed in (5), is used to describe system equity. The deviation considers travelers of different OD pairs (i.e. $w \in W$). Thus, the spatial dimension of equity is captured. In addition, the deviation considers travelers using different vehicle types (i.e. $m \in M$), which are likely to be correlated with travelers' socioeconomic characteristics. As such, the social dimension of equity is also incorporated. Furthermore, because μ's can be compared between networks, the metric allows for inter-network comparison of equity.

$$\bar{\mu} = \sum_w \left(\mu_{\mathrm{HV}}^w \frac{D_{\mathrm{HV}}^w}{D} + \mu_{\mathrm{CAV}}^w \frac{D_{\mathrm{CAV}}^w}{D} \right) \tag{4}$$

$$\max_{m \in M, w \in W} |\mu_m^w - \bar{\mu}| \tag{5}$$

The equity-side objective is to minimize the maximum deviation of any μ_m^w value across all OD pairs and both vehicle types from the system average $\bar{\mu}$, by selecting an appropriate CAV lane deployment scheme:

$$\min_{\boldsymbol{y}} \max_{m \in M, w \in W} |\mu_m^w - \bar{\mu}| \tag{6}$$

where $\boldsymbol{y}$ is a vector of binary decision variables indicating whether a specific lane of a specific link is converted to a CAV lane. The precise definition of $\boldsymbol{y}$ is introduced next.

3.3. Determining optimal CAV lane deployment

In this subsection, we formulate a bi-level bi-objective program to determine the optimal CAV lane deployment considering both system efficiency and equity. The bi-level program characterizes the process that a CAV infrastructure planner, when determining what HV lanes to convert into dedicated CAV lanes, anticipates how travelers would respond by adjusting their route choices, resulting in traffic redistribution in the network. Thus, the upper level is a bi-objective optimization problem, while the lower level is characterized by a multi-class traffic network equilibrium with CAV and HV vehicle types. Below we detail how the two levels are specified.

3.3.1. Upper level

The upper-level decision facing the CAV infrastructure planner is on what lanes to be converted to dedicated CAV lanes. We introduce binary variable y_a^i. to characterize the lane conversion decision. In y_a^i, $i \in I_a$. where I_a is the set of lanes on link $a \in \hat{\mathcal{A}}$. Lane $i \in I_a$. on physical link a. is converted to a dedicated CAV lane if $y_a^i = 1$. The lane is not converted if $y_a^i = 0$.

Following the link definition in Section 3.1, the dedicated CAV lane(s) on link $a \in \hat{\mathcal{A}}$. form virtual link $a' \in \hat{\mathcal{A}}_1$. . The remaining HV lane(s) on link a. form virtual link $a'' \in \hat{\mathcal{A}}_2$. To characterize the capacity of a virtual link, we use $\bar{\mathbb{C}}$ to denote the capacity of a single HV lane, and $\hat{\mathbb{C}}$ to denote the capacity of a single CAV lane. A CAV lane is expected to have a higher capacity than an HV lane as CAVs can travel closer together by leveraging real-time communications between vehicles (Chen et al. 2017; Lu et al. 2020). Tientrakool, Ho, and Maxemchuk (2011) showed that the capacity of a CAV lane can be nearly three times the capacity of a conventional lane.

On other hand, the capacity of an HV lane is considered invariant with a mix of HV and CAV traffic. We note that some CAV research argues that the capacity of a road link increases with the penetration of CAVs (Noruzoliaee, Zou, and Liu 2018; Wang et al. 2021). The argument was made by assuming an ideal driving environment where CAVs can precisely perceive their surroundings and make timely decisions and HV drivers are rational and do not extend their car-following distance in the presence of CAVs. However, such an ideal driving environment may not be realized (Do, Rouhani, and Miranda-Moreno 2019; Li et al. 2020; Ye and Yamamoto 2018). In practice, CAVs can be prohibited from traveling in very short headways on HV lanes, for safety reasons in mixed traffic (Chen, Wang, and Meng 2019). When following an HV, a CAV may even need additional time to react (Milanés and Shladover 2014). Considering these, we follow the literature (Chen, Wang, and Meng 2019; Milanés and Shladover 2014; Zhu et al. 2023) and assume invariant capacity for HV lanes.

Ts, the capacity of a physical link a with some lane(s) converted to dedicated CAV lane(s) consists of two parts: the capacity of the dedicated CAV lane(s) ($\Lambda_{a'}$) and the capacity of the remaining lanes ($\Lambda_{a''}$), as shown in (7). $\Lambda_{a'}$ is proportional to the number of dedicated CAV lanes on the link (which is $\sum_{i\in I_a} y_a^i$). $\Lambda_{a''}$ is proportional to the number of remaining HV lanes (which is $Y_a - \sum_{i\in I_a} y_a^i$; Y_a is the total number of lanes on the link).

$$\Lambda_{a'} = \hat{\mathbb{C}} \sum_{i\in I_a} y_a^i \qquad \forall\, a' \in \hat{\mathcal{A}}_1\ . \tag{7}$$

$$\Lambda_{a''} = \bar{\mathbb{C}}\left(Y_a - \sum_{i\in I_a} y_a^i\right) \quad \forall\, a'' \in \hat{\mathcal{A}}_2. \tag{8}$$

The objective of the optimal CAV lanes deployment problem are to (1) minimize system travel cost (efficiency), and (2) minimize the maximum deviation of any μ_m^w. from its system-level mean (equity), by deciding on what to be converted for dedicated CAV use while anticipating traffic response to the lane conversion:

$$\min_{y}\left\{ \sum_{m\in M}\sum_{a\in\mathcal{A}} c_a^m v_a^m, \quad \max_{m\in M, w\in W} |\mu_m^w - \bar{\mu}| \right\}. \tag{9}$$

$$\text{s.t.} \sum_{i\in I_a} y_a^i < Y_a \quad \forall\, a \in \hat{\mathcal{A}} \tag{10}$$

where $\boldsymbol{y} = \{y_a^i\}$, $\forall i \in I_a$, $a \in \hat{\mathcal{A}}$. Given a CAV lane deployment scheme, c_a^m. and v_a^m. will come from the equilibrium traffic flow at the lower level. Constraint (10), which is termed lane conversion constraint, stipulates that at least one HV lane is kept on any link $a \in \hat{\mathcal{A}}$. By doing so, HVs can always travel on any link.

3.3.2. Lower level

The lower level of the bi-level program characterizes traffic distribution on the network given a CAV lane deployment scheme, following Wardrop's first principle (Wardrop 1952). To do so, we use $f^r_{w,m}$ to denote traffic flow of vehicle type m on path (route) r of OD pair w. $r \in R^m_w$, where R^m_w denotes the set of paths for vehicle type m connecting OD pair w. The traffic flow conservation in the network is specified as follows:

$$\sum_{r \in R^m_w} f^r_{w,m} = D^w_m \quad \forall\ m \in M,\ w \in W \tag{11}$$

$$f^r_{w,m} \geq 0 \quad \forall\, m \in M,\ w \in W,\ r \in R^m_w \tag{12}$$

Equation (11) expresses that the sum of traffic flows for vehicle type m on all paths of an OD pair w, which equals the OD pair's travel demand for the vehicle type. Constraint (12) ensures that the traffic flow of a vehicle type on a path is always non-negative.

We specify the travel time on a link based on the Bureau of Public Roads (1964) function. For a link $a \in \bar{\mathcal{A}}$ which has only HV lanes, travel time on the link is computed as:

$$t_a = t^{\mathrm{HV}}_a = t^{\mathrm{CAV}}_a = t^0_a \left[1 + \alpha \left(\frac{v_a}{\Lambda_a} \right)^{\beta} \right] \quad \forall\, a \in \bar{\mathcal{A}} \tag{13}$$

where t_a denotes travel time on link a. The link may accommodate a mixed traffic of HVs and CAVs. Thus, the travel time of HVs and the travel time of CAVs on the link, t^{HV}_a and t^{CAV}_a, are the same and equal to t_a. t^0_a is the free-flow travel time on link a. v_a is vehicle flow on the link and is the sum of HV flow and CAV flow on the link: $v_a = v^{\mathrm{HV}}_a + v^{\mathrm{CAV}}_a$. Λ_a is the capacity of the link. α and β are parameters.

A link $a \in \hat{\mathcal{A}}$ can have both dedicated CAV lanes and HV lanes. In this case, travel time on the link needs to be calculated differently on the corresponding virtual links:

$$t_{a'} = t^{\mathrm{CAV}}_{a'} = t^0_a \left[1 + \alpha \left(\frac{v^{\mathrm{CAV}}_{a'}}{\Lambda_{a'}} \right)^{\beta} \right] \quad \forall\, a' \in \hat{\mathcal{A}}_1 \tag{14}$$

$$t_{a''} = t^{\mathrm{HV}}_{a''} = t^{\mathrm{CAV}}_{a''} = t^0_a \left[1 + \alpha \left(\frac{v^{\mathrm{HV}}_{a''} + v^{\mathrm{CAV}}_{a''}}{\Lambda_{a''}} \right)^{\beta} \right] \quad \forall\, a'' \in \hat{\mathcal{A}}_2 \tag{15}$$

For a physical link $a \in \hat{\mathcal{A}}$, if the corresponding virtual links a' and a'' both have CAV flows, then it must be that $t^{\mathrm{CAV}}_{a'} = t^{\mathrm{CAV}}_{a''}$, which means $t_{a'} = t_{a''}$. This is because otherwise, some CAVs would switch from one lane type to the other lane type, which would violate equilibrium. It is also possible that $a'' \in \hat{\mathcal{A}}_2$ does not have CAV flow. In other words, all CAVs on the physical link a travel on virtual link a'. If only a' has CAV flows, then $t_{a'} \leq t_{a''}$. because otherwise, some CAVs would switch from using a' to a'', which would also violate equilibrium. As $\Lambda_{a'}$ and $\Lambda_{a''}$. depend on y^i_a (as shown in Equation (7)–(8)), the travel time on the two virtual links of a physical link $a \in \hat{\mathcal{A}}$ is a function of the CAV lane conversion decisions.

For each of the two vehicle types, vehicle flow on a link follows the link-path relationship of Equation (16). The vehicle flow on a link is the sum of vehicle flows of the two vehicle types on the link (Equation (17)).

$$v_a^m = \sum_{w \in W} \sum_{r \in R_w^m} \delta_{a,r}^{m,w} f_{w,m}^r \quad \forall\, a \in \mathcal{A}, m \in M \tag{16}$$

$$v_a = \sum_{m \in M} v_a^m \quad \forall\, a \in \mathcal{A} \tag{17}$$

where $\delta_{a,r}^{m,w}$ is a 0–1 indicator of link-path incidence. It takes value one if link a is on path r of OD w for vehicle type m, and 0 otherwise.

We consider that travelers make route choice decisions based on their generalized travel cost, which includes not only travel time but out-of-pocket money. The generalized travel cost of travelers using vehicle type m on path r of OD w, denoted by $c_{w,m}^r$, is expressed in Equations (18)–(19). In Equation (18), the generalized travel cost of travelers using a vehicle type on a path is the sum of generalized travel cost on the links traversed by the path. Equation (19) specifies the generalized travel cost on a link for travelers using a vehicle type, which follows Noruzoliaee, Zou, and Liu (2018).

$$c_{w,m}^r = \sum_a \delta_{a,r}^{m,w} c_a^m \quad \forall\, m \in M, w \in W, r \in R_w^m \tag{18}$$

$$c_a^m = \eta_m t_a^m + \frac{\kappa_{m,1}\kappa_{m,2}}{\kappa_{m,3}\kappa_{m,4}\kappa_{m,5}} \rho_m l_a + \frac{VC_m}{\kappa_{m,5}} l_a \quad \forall\, a \in \mathcal{A},\ m \in M \tag{19}$$

In Equation (19), the first term on the right-hand side is travel time cost. The second term corresponds to the vehicle depreciation cost. The third term corresponds to the variable vehicle operating cost. Specifically, for a vehicle of type m, η_m is VOT of travelers using the vehicle type. ρ_m is the vehicle purchase price. $\kappa_{m,1}$ is a scale factor scaling vehicle price by taking further consideration the overhead costs (e.g. tax and registration fee). $\kappa_{m,2}$ is a proportion factor denoting the portion of the vehicle price value loss at the end of the vehicle's lifetime, as a result of depreciation. The average vehicle lifetime, measured in years, is denoted by $\kappa_{m,3}$. The average travel distance of a vehicle in a year is denoted by $\kappa_{m,4}$. The average occupancy of a vehicle is denoted by $\kappa_{m,5}$. l_a is the length of link a. VC_m denotes the unit variable operating cost of vehicle type m, in $/kilometer. The variable cost includes items such as fuel, maintenance, and insurance.

Following Yang and Huang (2004), the equilibrium condition for the multi-class user equilibrium with generalized travel cost can be written as follows:

$$f_{w,m}^r (c_{w,m}^r - C_w^m) = 0 \quad \forall\, m \in M, w \in W,\ r \in R_w^m \tag{20}$$

$$c_{w,m}^r - C_w^m \geq 0 \quad \forall\, m \in M, w \in W,\ r \in R_w^m \tag{21}$$

$$f_{w,m}^r \geq 0 \quad \forall\, m \in M, w \in W,\ r \in R_w^m$$

$$\sum_{r \in R_w^m} f_{w,m}^r = D_m^w \quad \forall\, m \in M, w \in W$$

where C_w^m is the minimum generalized travel cost by vehicle type m for OD pair w. The last two expressions are not numbered as they are already numbered earlier as (11) and (12). To solve the multi-class user equilibrium, we consider its equivalent optimization model. Specifically, we first re-express Equation (18) as a generalized travel time equation:

$$c^r_{w,m} = \sum_a \left\{ t^m_a + \frac{1}{\eta_m}\left(\frac{\kappa_{m,1}\kappa_{m,2}}{\kappa_{m,3}\kappa_{m,4}\kappa_{m,5}}\rho_m l_a + \frac{VC_m}{\kappa_{m,5}} l_a \right) \right\} \delta^{m,w}_{a,r} \quad \forall\ m \in M, w \in W,\ r \in R^m_w \tag{22}$$

Based on Equation (22), we formulate the following minimization problem for the CAV lane deployment problem:

$$Z(v^m_a) = \min \sum_a \int_0^{v_a} t_a(x)dx + \sum_a \sum_m v^m_a \frac{1}{\eta_m}\left(\frac{\kappa_{m,1}\kappa_{m,2}}{\kappa_{m,3}\kappa_{m,4}\kappa_{m,5}}\rho_m l_a + \frac{VC_m}{\kappa_{m,5}} l_a \right) \tag{23}$$

s.t. (11), (12), (16), and (17)

For brevity, we use U_m to denote $\frac{\kappa_{m,1}\kappa_{m,2}}{\kappa_{m,3}\kappa_{m,4}\kappa_{m,5}}\rho_m + \frac{VC_m}{\kappa_{m,5}}$, which captures the per unit distance out-of-pocket travel cost. Using the first-order Karush-Kuhn-Tucker (KKT) conditions of the above minimization problem, the equilibrium conditions with respect to general travel time can be derived:

$$\sum_a t^m_a \delta^{m,w}_{a,r} + \sum_a \frac{1}{\eta_m} l_a U_m \delta^{m,w}_{a,r} = \lambda^m_w \quad \text{if } f^r_{w,m} > 0 \quad \forall\, m \in M, w \in W,\ r \in R^m_w \tag{24}$$

$$\sum_a t^m_a \delta^{m,w}_{a,r} + \sum_a \frac{1}{\eta_m} l_a U_m \delta^{m,w}_{a,r} \geq \lambda^m_w \quad \text{if } f^r_{w,m} = 0 \quad \forall\, m \in M, w \in W,\ r \in R^m_w \tag{25}$$

where λ^m_w is the Lagrange multiplier corresponding to Equation (11). Multiplying both sides of (24)–(25) by η_m, we obtain:

$$\sum_a \eta_m t^m_a \delta^{m,w}_{a,r} + \sum_a l_a U_m \delta^{m,w}_{a,r} = \eta_m \lambda^m_w \quad \text{if } f^r_{w,m} > 0 \quad \forall\, m \in M, w \in W,\ r \in R^m_w \tag{26}$$

$$\sum_a \eta_m t^m_a \delta^{m,w}_{a,r} + \sum_a l_a U_m \delta^{m,w}_{a,r} \geq \eta_m \lambda^m_w \quad \text{if } f^r_{w,m} = 0 \quad \forall\, m \in M, w \in W,\ r \in R^m_w \tag{27}$$

The left-hand side of Equations (26)–(27) is the path travel cost $c^r_{w,m}$. On the right-hand side, λ^m_w is the corresponding Lagrangian multiplier. Equations (26)–(27) indicate that $c^r_{w,m}$ is equal to traveler VOT η_m times λ^m_w when there is traffic flow on the path; the path travel cost is no less than $\eta_m\lambda^m_w$ when there is no traffic flow on the path. Thus, (26)–(27) is equivalent to (20)–(21) and (12), with $\eta_m\lambda^m_w$ representing the minimum OD travel cost C^m_w. In other words, the solution of the minimization problem of (23) (subject to constraints (11), (12), (16), and (17)) is a solution for the multi-class user equilibrium with generalized travel cost. The minimization problem can be solved by the well-known Frank-Wolfe algorithm (Frank and Wolfe 1956). A detailed proof of the equivalency between the KKT conditions of the minimization problem and (20)–(22) is relegated to Appendix.

As a final note for the lower-level formulation, it should be noted that in formulating the lower-level problem, the demand on an OD pair is assumed fixed. By assuming so, we intend to focus our study on the relatively *short-term* effects of CAV lane deployment on system efficiency and equity *given* the existing travel demand. On the other hand, as the adoption of CAVs increases, the OD demand patterns are likely to evolve in the longer term. Incorporating such CAV adoption would give rise to new modeling challenges. First, the adoption of CAVs will depend not only on the travel cost of using CAV, but a number of other economic, sociodemographic, and attitudinal factors (Chen et al. 2022; Talebian and Mishra 2018). Thus, how to appropriately characterize CAV adoption will be a separate study itself. Second, even with an adoption function, how to integrate it into the existing modeling framework could involve considerable effort. For example, one possibility could be to assume that CAV adopters switched from using HVs. Then, a binomial Logit model should be specified to capture traveler vehicle type choice and added to the multi-class network equilibrium formulation. Understanding the best ways to characterize and incorporate CAV adoption into the lower-level problem will be left for future research.

4. Solution algorithm

The CAV lanes deployment problem can be viewed as a type of discrete network design problem (Farahani et al. 2013), for which finding an exact solution is generally NP-hard and challenging (Yu et al. 2015). Considering further that the problem has two objectives to deal with, we propose to solve our problem by a customized algorithm, termed NSGA-II-VNS, which leverages the complementary strengths of NSGA-II in global search for bi-objective optimization and VNS in local search while we seek the optimal solution, i.e. optimal CAV lane deployment scheme. NSGA-II, initially proposed by Deb et al. (2002), is a classical algorithm for solving multi-objective optimization. Simulating natural evolutionary processes, NSGA-II characterizes solutions as chromosomes. In our context, each element in a chromosome corresponds to a convertible lane, and is binary indicating whether the lane is converted to a CAV lane. Thus, the length of a chromosome is equal to the number of convertible lanes. To illustrate, consider a network consisting of five convertible lanes. Chromosome $\mathcal{C} = [0,\ 1,\ 1,\ 0,\ 0]$ denotes a solution with lanes 2 and 3 converted to dedicated CAV lanes.

While NSGA-II copes with multi-objective optimization, it is rooted in genetic algorithm which is generally good at diversifying the solution space by considering and evaluating a population of solutions that evolve over generations (Mohammadi, Jula, and Tavakkoli-Moghaddam 2019). On the other hand, genetic algorithm is less good in intensifying search in local regions. In our paper, we try to mitigate this weakness by hybridizing NSGA-II with VNS, to balance global exploration with local exploitation during the evolutionary process. VNS, which was initially proposed by Mladenović and Hansen (1997) and has since been widely employed in solving complex combinatorial and global optimization problems (e.g. see the review of Hansen, Mladenović, and Moreno Pérez (2010)), relies on the idea of constructing and performing local search for better solutions over different neighborhood structures.

By hybridizing NSGA-II with VNS, we replace the crossover operation with multiple neighborhood searches. Specifically, the following manifold neighborhood search structure is employed:

(1) Left Insert (Figure 3(a)): Randomly select a lane (Location 1) from the current CAV lane deployment scheme, and randomly pick another position (Location 2) on the left of Location 1. Then, insert Location 1 to the left of Location 2.

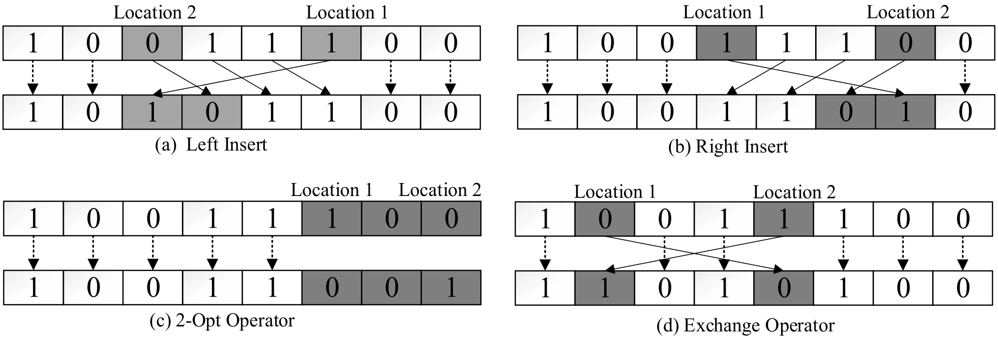

Figure 3. Neighborhood search structures.

(2) Right Insert (Figure 3(b)): Randomly select a lane (Location 1) from the current CAV lane deployment scheme, and randomly pick another position (Location 2) on the right of Location 1. Then, insert Location 1 to the right of Location 2.
(3) 2-Opt Operator (Figure 3(c)): Randomly select two lanes from the current CAV lane deployment scheme. Then reverse the order of positions between the two lanes.
(4) Exchange Operator (Figure 3(d)): Randomly select two lanes from the current CAV lane deployment scheme. Exchange values of the two selected lanes.

Note that a random number $\rho \in (0, 1)$ is first drawn, to determine whether the above VNS is performed on a chromosome. If the ρ value is below a prespecified threshold value, VNS is performed. If the ρ value is above the threshold value, then a random solution is generated instead. The detailed algorithmic steps of NSGA-II-VNS is shown in Table 1.

In implementing the NSGA-II-VNS algorithm, whenever a chromosome is generated, constraint (10) always needs to be respected. Specifically, in step 1 of the algorithm, if a randomly generated chromosome violates constraint (10), we discard the chromosome, and randomly generate another one. We keep doing this until a feasible chromosome is obtained. Similarly for the random chromosome generation in step 5 of the algorithm. In

Table 1. Detailed steps of the NSGA-II-VNS algorithm.

Step 1	*Initialization.* Initialize the generation counter $g = 1$. Set the population size to $2N$. Generate randomly the first population of chromosomes, denoted as $P_g = P_1$.
Step 2	*Traffic assignment.* For each chromosome in the current population P_g, perform multi-class traffic assignment based on Frank-Wolfe algorithm, to obtain the equilibrium traffic flow on the network.
Step 3	*Compute objective values.* Given the equilibrium traffic flow, compute system travel cost and equity for each chromosome in P_g. Based on the computed system travel cost and equity values, perform non-dominated sorting of the chromosomes and compute crowding distance (see Deb et al. 2002) for each chromosome.
Step 4	*Preserve elite chromosomes.* With the sorting and crowding distance computation results, pick $N/2$ chromosomes by tournament selection. The picked chromosomes constitute a new population P_g^1.
Step 5	*Variable neighborhood search.* For each chromosome in p_g^1, generate a random value $\rho \in (0, 1)$. . If $\rho < \rho_c$ which is the threshold for performing VNS, perform VNS to generate four new chromosomes. Otherwise, randomly generate a chromosome. The generated chromosomes constitute another new population P_g^2.
Step 6	*Perform elite selection operations.* Perform non-dominated sorting to pick $2N$ chromosomes from the combined $P_g^1 + P_g^2$ population. These $2N$ picked chromosomes form population p_{g+1}.
Step 7	*Determine whether to stop or move to the next iteration.* If $g + 1$ is no greater than the maximum number of generations to perform, set $g = g + 1$. Go back to step 2 and repeat. If $g + 1$ reaches the maximum number of generations, perform only steps 2–3 to obtain Pareto solutions. Then stop.

step 5, we also keep performing the search until a feasible chromosome is found for each neighborhood search structure under VNS.

In performing step 5, we set ρ_c to 0.9, which means a large probability that VNS will be performed. In other words. number of generated solutions, which constitute p_g^2, is likely to be closer to $2N$. rather than $N/2$, the latter resulting from simply doing random chromosome generation. Consequently, the combined size of p_g^1. and p_g^2 is likely to be greater than $2N$, making it necessary to select $2N$ chromosomes out of the combined p_g^1 and p_g^2.

5. Numerical experiments

In this section, we perform numerical experiments of the bi-level bi-objective optimization program and the solution algorithm on two networks. The first is a modified Nguyen-Dupuis network, where a base case and alternative scenarios are investigated. Then, we examine CAV lane deployment on a real-world large-scale network of south Florida. The numerical experiments are run on a PC with Intel(R) Core(TM) i7 CPU @ 2.60 GHz with 32 GB RAM.

5.1. Experiments on Nguyen-Dupuis network

The modified Nguyen-Dupuis network used in our experiments has 13 nodes, 19 links, and nine OD pairs (Figure 4). The OD information is listed in Table 2. The main modeling parameters are drawn from the Chen et al. (2016) and Noruzoliaee, Zou, and Liu (2018), as presented in Table 3. In particular, the value difference in the unit variable cost parameters VC_m, $m \in \{\text{HV, CAV}\}$. reflects additional maintenance cost associated with the CAV technologies as well as reduced insurance and fuel cost when using CAVs (Noruzoliaee, Zou, and Liu 2018). The detailed attributes of the network are presented in Table 4. The capacity of a dedicated CAV lane is considered 2.5 times the

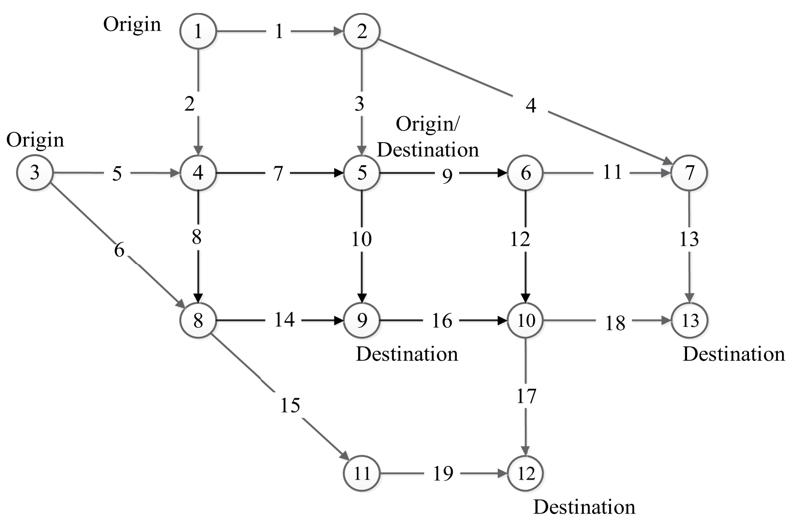

Figure 4. Nguyen-Dupuis network.

Table 2. OD demand of the Nguyen-Dupuis network.

Number	1	2	3	4	5	6	7	8	9
OD pair	(1–12)	(1–13)	(3–13)	(3–12)	(1–5)	(3–5)	(3–9)	(5–12)	(3–13)
Demand	2,000	2,000	2,000	1,600	600	1,000	1,600	1,400	1,200

Table 3. Values for main modeling parameters.

Parameter	Value		Parameter	Value	Parameter	Value
	CAV	HV				
η_m (\$/min)	0.4	0.5	$\kappa_{m,1}$	5.1	$\kappa_{m,4}$	20,000
VC_m (\$/km)	0.284	0.264	$\kappa_{m,2}$	0.9	$\kappa_{m,5}$	1
ρ_m (\$)	28,000	20,000	$\kappa_{m,3}$	10		

Table 4. Link attributes of the Nguyen-Dupuis network.

Link	t_a^0	Number of lanes	Capacity	Length (km)	Link	t_a^0	Number of lanes	Capacity	Length (km)
1	9	3	2,400	5.4	11	5	2	1,600	3.0
2	7	4	4,000	4.2	12	9	4	3,200	5.4
3	7	3	3,000	4.2	13	9	3	2,400	5.4
4	14	2	2,000	8.4	14	10	4	6,000	6.0
5	9	3	3,000	5.4	15	9	2	3,000	5.4
6	12	3	4,500	7.2	16	6	4	4,000	3.6
7	3	4	5,200	1.8	17	5	3	3,000	3.0
8	9	3	3,900	5.4	18	9	4	6,000	5.4
9	5	3	2,400	3.0	19	11	3	4,500	6.6
10	13	3	4,500	7.8					

capacity of an HV lane. For each OD pair, travel demand is evenly split between CAVs and HVs. With the exception of comparing the Pareto frontiers by NSGA-II-VNS and enumeration in Section 5.1.1, each link is assumed to have one convertible lane. In implementing NSGA-II-VNS, the population size is 20 (the only exception is when NSGA-II-VNS is compared with NA-II in Figure 8. There the population size is set to 50 to generate more solutions on Pareto frontiers.). The number of generations is set to 50.

5.1.1. Base case

In the base case, we follow the network setup in Chen, Wang, and Meng (2019) (which is also for AV lane deployment) and consider seven links each of which has one convertible lane, as shown in Figure 5. Considering a subset of the links with convertible lanes allows us to enumerate all possible CAV lane deployment schemes (in total $2^7 = 128$ schemes) and evaluate the effectiveness of the NSGA-II-VNS algorithm and the quality of the solutions obtained in a reasonable amount of time. Nonetheless, it is worth noting that the proposed model and solution algorithm are generic and can solve problems with alternative network setups. The system travel cost and equity for each of the 128 schemes are displayed as blue dots in Figure 6. Note that the number of dots is less than 128, as some schemes have identical system travel cost and equity. The non-dominated solutions are connected in the small subfigure in Figure 6, forming the true Pareto frontier. The three orange dots (labeled as ‘Scheme 1’, ‘Scheme 2’, and ‘Scheme 3’) are solutions obtained from NSGA-II-VNS. These orange dots overlap with true Pareto solutions

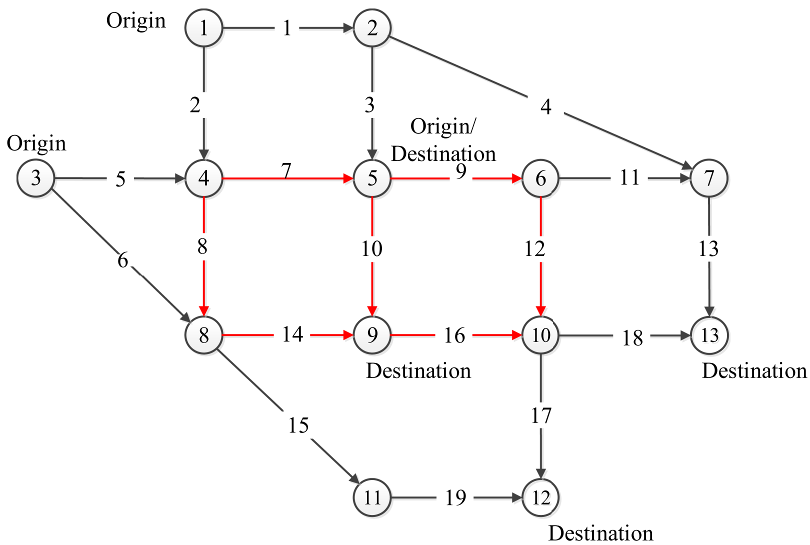

Figure 5. The Nguyen-Dupuis network considered (each red link allows one lane to be converted to a dedicated CAV lane).

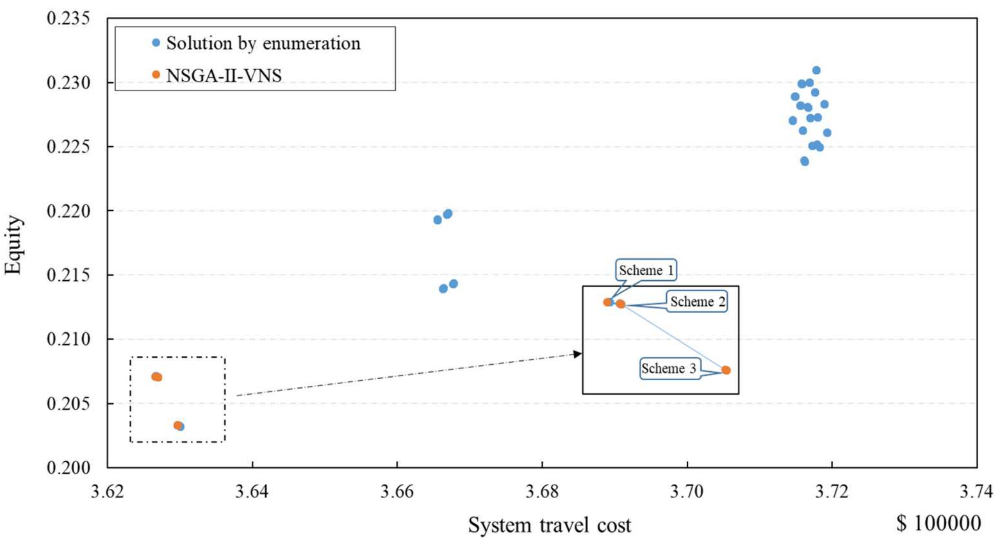

Figure 6. Pareto frontiers obtained based on NSGA-II-VNS and enumeration.

from enumeration, suggesting the effectiveness of NSGA-II-VNS. Figure 7 shows the CAV lane deployment associated with the three solutions from NSGA-II-VNS.

Note that the extent of convergence of the solutions obtained by NSGA-II-VNS to the solutions on the true Pareto frontier can be quantified by the convergence metric Υ (Deb et al. 2002). As illustrated in Figure 8, the black circles are the solutions on the true Pareto frontier. The red circles are the solutions obtained by NSGA-II-VNS. For each red solution, we measure the closest Euclidean distance to any black solution on the true

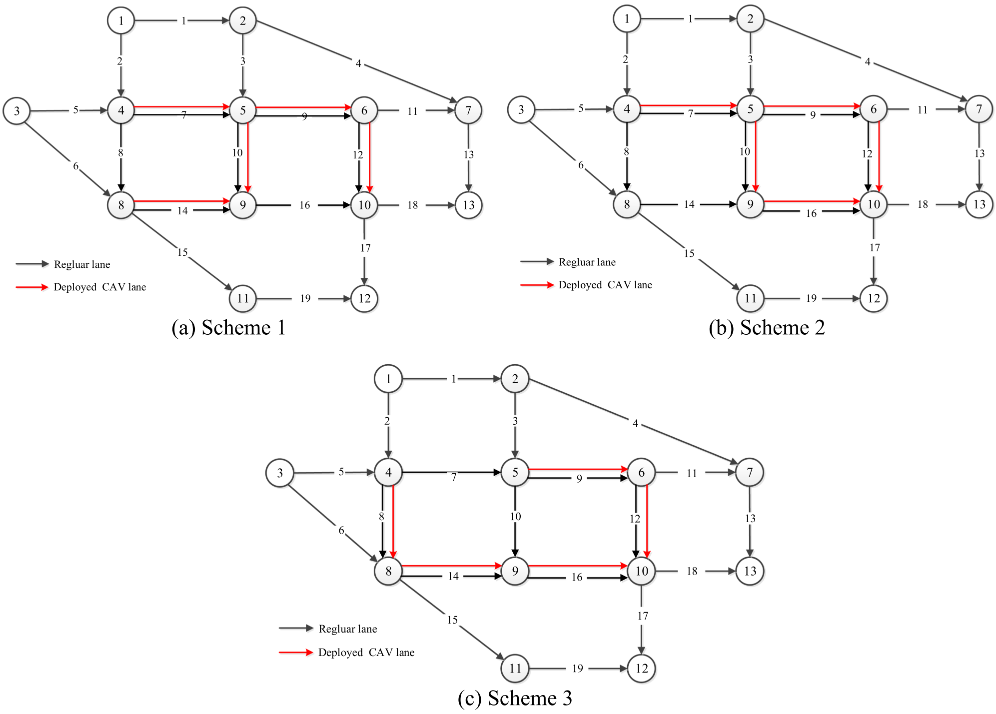

Figure 7. CAV lane deployment results of the three Pareto solutions obtained from NSGA-II-VNS (each red link indicates that an actually deployed CAV lane).

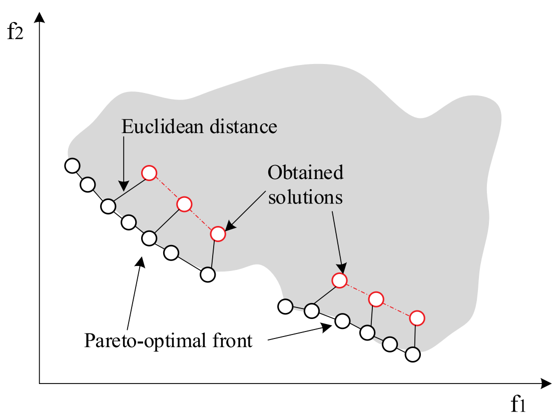

Figure 8. Illustration of computing the convergence metric value for NSGA-II-VNS.

Pareto frontier. The average of the distances for all the red solutions gives the value of Υ. In our case, because the NSGA-II-VNS solutions overlap with the true Pareto solutions, $\Upsilon = 0$, i.e. the NSGA-II-VNS algorithm leads to converging results.

Recall that an important feature of NSGA-II-VNS is the hybridization of NSGA-II with VNS. Next, we compare the Pareto frontiers produced by NSGA-II-VNS and NSGA-II. Figure 9 shows the resulting Pareto frontiers. Clearly, NSGA-II-VNS produces

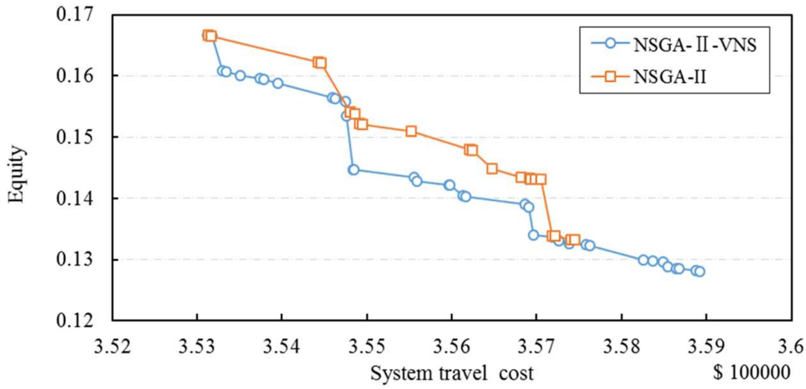

Figure 9. Pareto frontiers generated by NSGA-II-VNS and NSGA-II.

a better frontier which lies to the lower left of the frontier produced by NSGA-II. Therefore, augmenting NSGA-II with VNS does enhance the Pareto solution quality.

We observe that the Pareto frontiers in Figure 9 are not smooth. In other words, the tradeoff between system travel cost and equity varies depending on the level of system travel cost. For example, on the NSGA-II-VNS frontier, the equity value will experience a significant decrease – from 0.156 to 0.145 (or 7%) – when system travel cost increases slightly from $\$3.547 \times 10^5$ to $\$3.549 \times 10^5$ (or 0.03%). The implied equity elasticity with respect to system travel cost is $7\%/0.03\% = -246$. By contrast, the equity value decrease is much less as we continue increasing system travel cost from $\$3.548 \times 10^5$ to $\$3.569 \times 10^5$. The implied equity elasticity with respect to system travel cost at about -7.

We further observe that there can be multiple solutions on the NSGA-II-VNS frontier (similarly, on the NSGA-II frontier) that have almost the same system travel cost and equity. If the corresponding system travel cost and equity values are desired, one may ask which solution should be picked. For this, further looking at the cost of CAV lane conversion would be needed. The most preferred solution should be one that costs the least.

5.1.2. Alternative scenarios

We further investigate how system travel cost and equity change under alternative scenarios by varying travel demand, CAV price, CAV traveler VOT, and the available budget.

(1) **Travel demand.** We consider three alternative scenarios with the travel demand at 0.5, 2, and 4 times of the base travel demand. For these demand levels, the Pareto frontiers are presented in Figure 10. The Pareto frontier under the base demand is also presented as a reference. Not surprisingly, the system travel cost increases as travel demand increases. The cost increase is more than proportionate, which is attributed to the nonlinear impact of traffic flow on congestion, as characterized by the BPR form of the link travel time function.

We observe that it is more difficult to maintain equity as travel demand increases. In addition, the equity value range on a Pareto frontier expands as demand increases. For example, at 0.5 times base demand, the maximum and the minimum equity values are 0.107 and 0.083 (the difference is 0.024). When demand increases to four times the

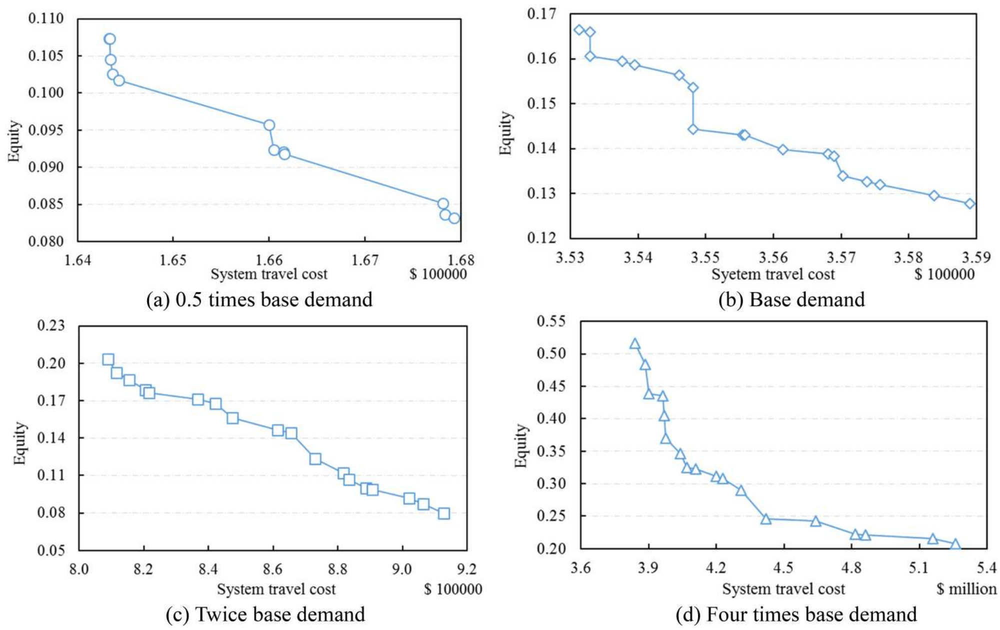

Figure 10. Pareto frontiers under four demand scenarios.

base demand, the maximum and the minimum equity values drastically increase to 0.517 and 0.207 (the difference is 0.310). Thus, the system becomes less equitable with more travelers.

To understand the cause of inequity as demand increases, the values of μ's, i.e. the generalized travel cost per unit OD distance defined in Equations (2)–(3), are plotted for each of the nine ODs and for CAV and HV travelers. For each demand level, we select the Pareto solution with the largest equity value (the most inequitable solution) to plot μ values. Figure 11 shows that when demand is low at 0.5 times the base demand, the μ values are more or less the same across ODs and between the two vehicle types. As demand increases to the base level, μ values across ODs begins to show disparities: OD pairs 5, 6, and 7 have the lowest μ values while OD pair 9 has the highest. The disparities become more noticeable when demand increases to twice the base demand. When demand increases further to four times the base demand, the equity gap between CAV and HV also appear. HV travelers will experience significantly greater travel cost per unit OD distance for most ODs. At one extreme, HV travelers of OD pair 4 would spend more than twice the average cost per unit OD distance of CAV travelers.

The above results clearly indicate that inequity stems from two sources. The first source is inequity among travelers of different ODs, which exhibits early as demand increases. The second source is inequity between travelers using CAVs vs. HVs. This inequity starts its effect later when demand is further increased. On the other hand, once showing the effect, the second source contributes greatly to the overall inequity.

(2) **CAV price.** The selling price of a CAV affects travel cost of CAV travelers. We investigate how the Pareto frontier changes as we have a different CAV price. Two alternative CAV prices, at 90% and 80% of the base level, are examined. While HVs

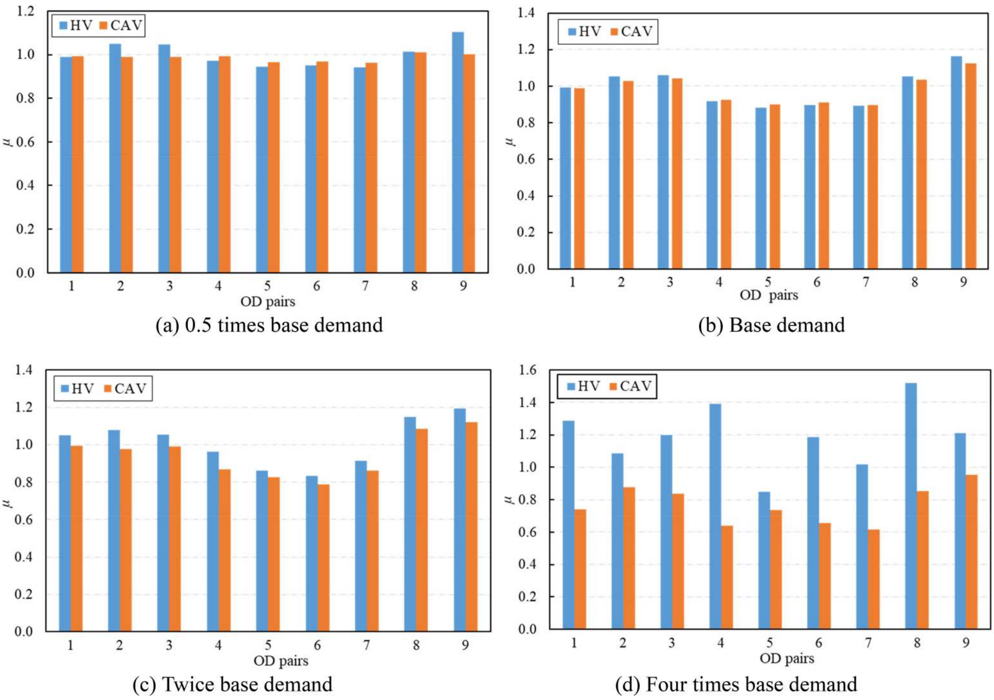

Figure 11. μ values for both CAV and HV travelers on each OD pair, under four demand scenarios.

might also respond to a lower CAV price, given the maturity of the HV technology we conjecture that the room of such a response would be limited. In the following, we keep HV price constant and focus on the effect of CAV price on the Pareto frontier.

Figure 12 shows that the two alternative frontiers and the frontier from the base case are similar in shape. As CAV becomes cheaper, a reduced system travel cost is expected,

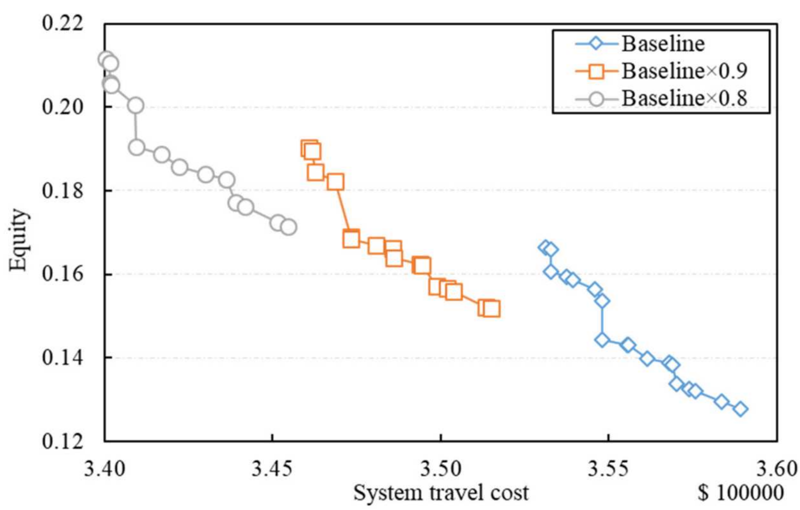

Figure 12. Pareto Frontiers with different CAV prices.

as evidenced by the leftward move of the frontier. Meanwhile, cheaper CAVs reduces the travel cost per unit OD distance, giving CAV travelers further cost advantage and widening the equity gap. This is evidenced by the upward move of the frontier. Thus, HV travelers will be negatively affected in terms of equitable travel. CAV infrastructure planners need to be cognizant of this. Actions may be needed to mitigate the inequity effect, for example, by subsidizing HV travelers. This will be explored in Section 5.1.3.

(3) **CAV traveler VOT.** CAV traveler VOT differs from HV traveler VOT due to the influence of two factors. First, as CAVs entail automation, less human interference is expected while traveling. Consequently, travelers could use a greater proportion of their in-vehicle time for other more productive or leisurely activities. This helps reduce CAV traveler VOT. Second, travelers who use CAVs are likely to be those who value their time more. Depending on which factor dominates, the net effect can be a lower or a higher CAV traveler VOT. Given that the base case VOT for CAV travelers is \$0.4/min, we explore four alternative values for CAV traveler VOT: \$0.2/min, \$0.3/min, \$0.5/min, and \$0.6/min. The resulting Pareto frontiers are reported in Figure 13.

A few observations are worth noticing. First, as CAV traveler VOT increases, system travel cost increases, which is not surprising as travel time cost is part of the system travel cost. Second, starting from the base value for CAV traveler VOT (\$0.4/min), either increasing or decreasing the VOT will push the Pareto frontier upward, i.e. widening the equity gap. This may result from the fact that increasing VOT makes CAV travelers worse off in their generalized travel cost compared to HV travelers, while decreasing the VOT does the opposite. The farther away the CAV traveler VOT from the base value, the greater the inequity. Third, if CAV travelers have a lower VOT, the Pareto frontier is smoother than if CAV travelers have a higher VOT, where a sudden drop is observed

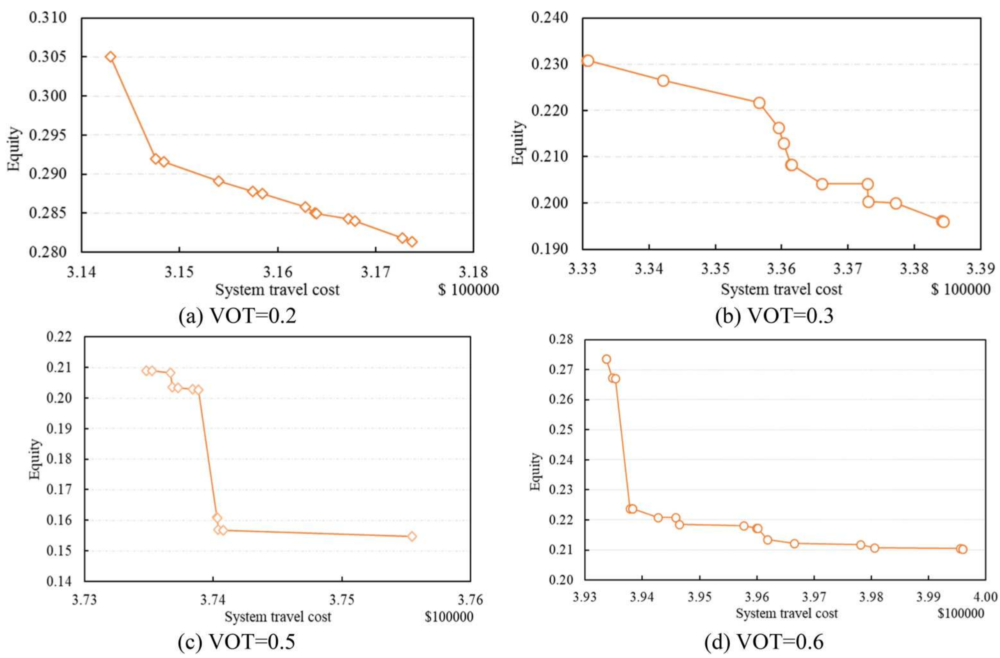

Figure 13. Pareto frontiers with different CAV traveler VOT values.

(see Figure 13(c and d)). In fact, under a higher VOT, a relatively small system travel cost can be achieved on the frontier while keeping equity at a low value.

Figure 14 plots the μ values for CAV and HV travelers on each OD pair. For a given CAV traveler VOT, the μ values again are based on the solution with the largest equity value on the Pareto frontier. We can see that as we increase the CAV traveler VOT, the μ values for CAV and HV travelers follow opposite changing directions: the values increase for CAV travelers and decrease for HV travelers, consistently across all OD pairs. When CAV traveler VOT = \$0.4/min, the μ values of the CAV and HV travelers are the closest, yielding the lowest equity value. Either increasing or decreasing the CAV VOT, the μ value difference between CAV and HV travelers will be widened, resulting in greater inequity. This echoes what we observe in Figure 13.

(4) **Available budget for CAV lane deployment.** An important factor affecting CAV lane deployment is how much budget is available. Conceptually, with a smaller budget, the Pareto frontier should be no better than with a larger budget. Four budget levels are tested: the first one with a base budget and the other three each with a portion of the base budget. The base budget is set to the maximum cost for CAV lane deployment and operation, i.e. the required cost meets all convertible lanes were converted and operation. In other words, having a base budget is equivalent to no budget constraint. Assuming a unit CAV lane conversion cost of \$100,000/lane-kilometer (Chen, Wang, and Meng 2019), the deployment cost budget is set to \$9,660,000. The operation cost of CAV lane come from infrastructure maintenance, technology maintenance, software and so on. Assuming the average annual operating costs of CAV lane is \$30,000 per kilometer per year and the average operating cycle of CAV lane is 10 years, the operation cost budget is set to \$28,980,000 (Greer et al. 2018; Kockelman et al. 2017; Smith et al. 2015). Thus, the base budget is \$38,640,000. The other three budget levels are set to 80%, 60%, and 40% of the base budget.

The budget constraint is incorporated in the upper level of the bi-level program:

$$\sum_{a\in\hat{\mathcal{A}}}\sum_{i\in I_a} u_a^i y_a^i \leq B \quad \forall a \in \hat{\mathcal{A}},\ i \in I_a \tag{28}$$

where u_a^i denotes the deployment and operation cost of CAV lane i on link a. Given the same unit lane cost, u_a^i can be simplified as u_a which is a linear function of link length.

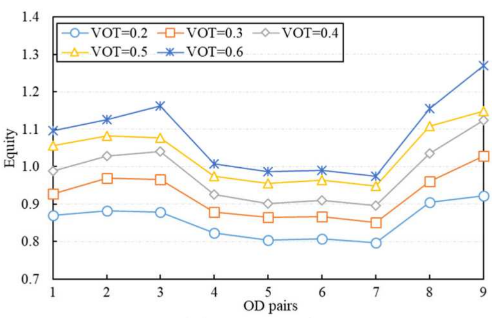

(a) CAV travelers

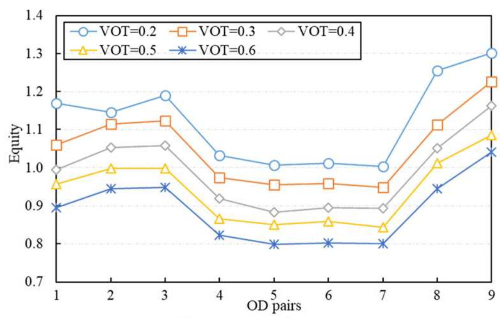

(b) HV travelers

Figure 14. μ values for CAV and HV travelers on each OD pair, with different CAV traveler VOTs.

With the budget constraint, performing NSGA-II-VNS needs to ensure that total cost of CAV lane deployment and operation for a chromosome always respects the budget constraint. Figure 15 shows the Pareto frontiers. We find that reducing the budget by up to 40% does not alter the shape of the frontiers much. As we further reduce the budget by 60%, the frontier becomes different: the middle and the upper parts of the froner move rightward, meaning greater system travel cost if we want to achieve the same level of equity. On the other hand, if we focus on achieving the best possible equity, reducing the base budget by 60% would still be okay, as the lower part of the frontier remains almost the same. Overall, constraining the budget seems to impact the best achievable system travel cost more than the best achievable equity.

5.1.3. Subsidizing HV travelers

The results in Section 5.1.2 show that as CAV becomes more popular and mature – characterized by higher demand, lower CAV price, and reduced CAV traveler VOT, the system travel cost will decrease. However, the system also becomes more inequitable between CAV and HV travelers. In this subsection, we explore the possibility of subsidizing HV travelers to mitigate the inequity.

We consider that subsidy to HV travelers is provided based on the distance traveled. Three subsidy levels are examined: \$0.05/km, \$0.12/km, and \$0.16/km. Figure 16(a) shows the Pareto frontiers with and without the subsidy. As HV travelers receive subsidy, system travel cost is decreased. Higher subsidy leads to smaller system travel cost, reflected in the leftward movement of the frontiers. For the impact of subsidy on equity, we first look at the frontier with \$0.05/km subsidy. Three solutions (in green) are picked from the frontier, with the μ values of all ODs and between CAV and HV travelers for the three solutions presented in Figure 16(b)–(d).

Because of the subsidy, HV travelers enjoy a smaller travel cost per unit OD distance than CAV travelers (with the only exception of OD pair 9, where the μ values for HV travelers are only slightly higher). If we continue providing more subsidies, HV travelers

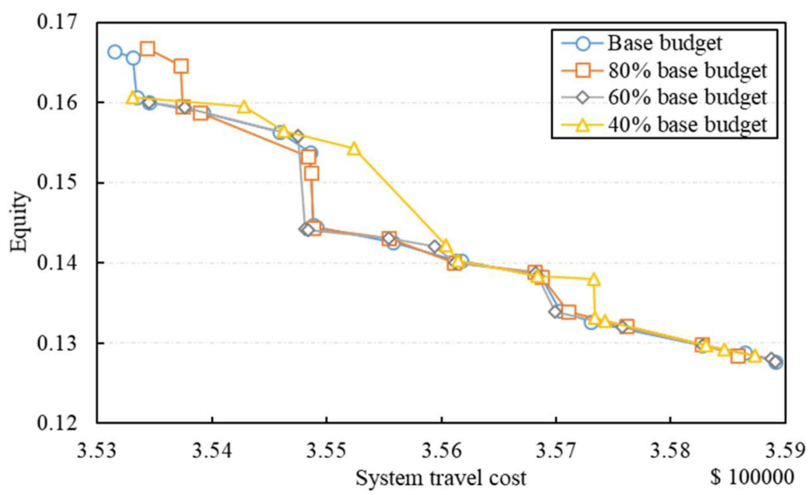

Figure 15. Pareto frontiers under different budget levels.

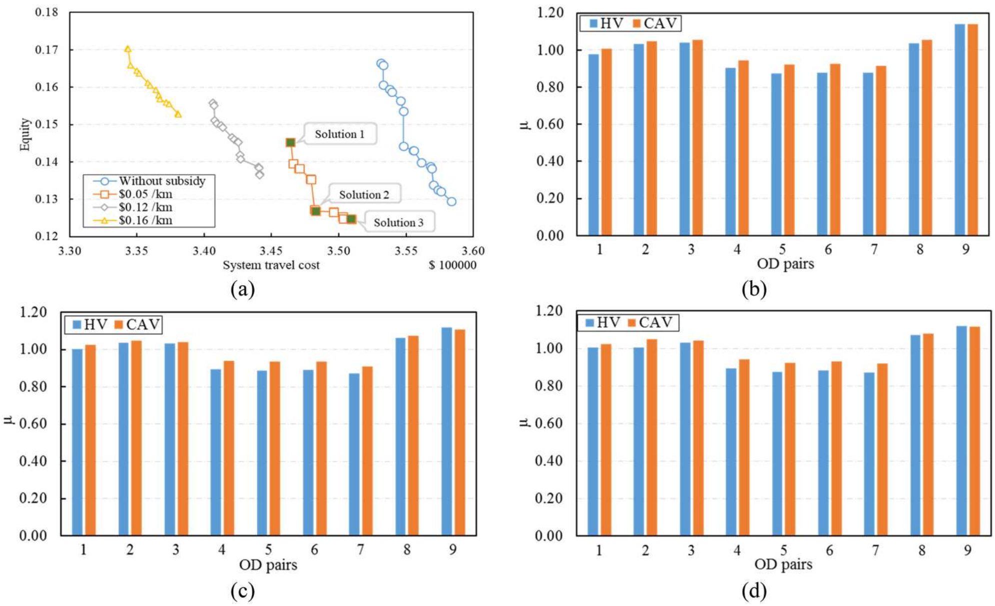

Figure 16. (a) Pareto frontiers with HV traveler subsidy; (b)–(d) μ values for CAV and HV travelers on each OD pair, for the three solutions (in green) on the Pareto frontier with a subsidy of \$0.05/km.

will become over-subsidized, with the travel cost per unit distance further below the cost for CAV travelers. This exacerbates inequity, as reflected in the upward movement of the frontiers in Figure 16(a).

The question of what subsidy level is appropriate depends on system parameter values, including those that define the alternative scenarios in Section 5.1.2. To this end, we construct Pareto frontiers with the parameter values leading to the most inequity, under each alternative scenario in Section 5.1.2: four times base demand, 80% base CAV price, and CAV traveler VOT at \$0.2/min. Figure 17 displays the frontiers.

Figure 17(a) shows that when travel demand is very high, adding more subsidy does not substantially improve system travel cost and equity, as the associated frontiers (in orange, grey, and yellow) are quite close to each other. Considering that higher travel demand means greater congestion, these frontiers suggest that in a highly congested network subsidy has limited effect on improving equity. By contrast, when CAV price is low (Figure 17(b)) and CAV traveler VOT is low (Figure 17(c)), more clear trends of simultaneous improvement on system travel cost and equity are observed. Thus, as CAV becomes more attractive because of cheaper price and lowered traveler VOT, more subsidy will help HV travelers reduce travel cost and consequently the equity gap between HV and CAV travelers.

As an additional examination, we compare the amount of subsidy with the reduction in system travel cost, which is the cost difference with and without the subsidy. Table 5 reports the results. In each row, the comparison is based on the solution that has the worst equity on the frontier. The last column of the table shows the ratio of system travel cost reduction to the amount of subsidy, which can be viewed as the 'returns' on subsidy.

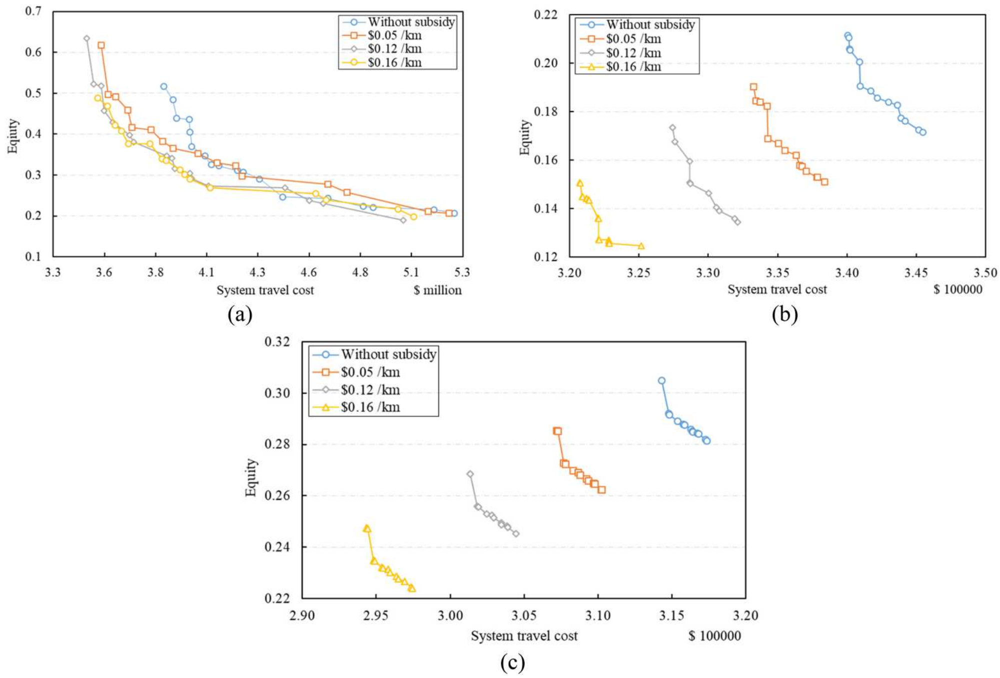

Figure 17. Pareto frontiers with HV traveler subsidy under three alternative scenarios: (a) four times base demand, (b) 80% base CAV price, and (c) CAV traveler VOT = \$0.2/min.

Table 5 shows three interesting points. First, as we increase the subsidy level, system travel cost keeps decreasing. For most of the scenario-subsidy level combinations, the returns on subsidy takes a value greater than one, justifying the use of subsidy to enhance system efficiency. On the other hand, the changing trends of the ratio are not monotonic. In the base case, the best ratio occurs at subsidy level \$0.05/km, which coincides with the best Pareto frontier based on equity as shown in Figure 16(a). For the other three scenarios, the subsidy level that achieves the best ratio is also at \$0.05/km, which however does not coincide with the best Pareto frontier based on equity as shown in Figure 17. Thus, subsidizing HV travelers at a level greater than \$0.05/km is

Table 5. Total subsidy, system travel cost reduction, and the ratio of the two under different subsidy levels and scenarios for the Nguyen-Dupuis network.

Scenario	Subsidy level (\$/km)	Total subsidy (I) (\$)	System cost reduction (II) (\$)	Ratio (II/I)
Base case	0.05	5,513	6,846	1.24
	0.12	11,036	12,542	1.14
	0.16	16,573	19,373	1.17
Four times base demand	0.05	22,754	27,753	1.22
	0.12	54,641	49,133	0.90
	0.16	72,467	77,303	1.07
80% base CAV price	0.05	5,221	6,843	1.31
	0.12	12,541	12,534	1.00
	0.16	16,740	19,363	1.16
CAV traveler VOT = \$0.2/min	0.05	5,247	6,306	1.20
	0.12	12,593	11,538	0.92
	0.16	16,792	17,851	1.06

less desirable from the economic return perspective. In particular for the scenarios of 80% base CAV price and CAV traveler VOT at $0.2/min, a large HV traveler subsidy will help improve equity, but this should be balanced with the economic returns of doing so.

5.1.4. The alternative measures for mitigating inequity

As an opposite of subsidizing HV travelers, one might also think of pricing CAV travelers to improve equity. A reasonable argument can be that a use fee be levied when CAVs use the dedicated CAV lanes, to recover the CAV lane conversion cost. In view of this, the effect of introducing a CAV lane use fee to mitigate inequity is explored. In addition, we propose a lane-access restriction strategy that all CAVs travel exclusively on CAV lanes when such lanes are present on a link and analyze the impact of this strategy on system equity.

5.1.4.1. CAV lane use fee. The effect of introducing a fee to CAV travelers for using dedicated CAV lanes is investigated. Such a fee can be justified to recover the CAV lane conversion cost. Three use fee levels are examined: $0.06/km, $0.12/km, and $0.17/km. The resulting Pareto frontiers, along with the Pareto frontier without a use fee, are shown in Figure B1(a). Similar to the subsidy investigation, we also investigate the Pareto frontiers with a use fee under three alternative scenarios: four times base demand, 80% base CAV price, and CAV traveler VOT at $0.2/min. The resulting Pareto frontiers (along with the Pareto frontier without a use fee) are displayed in Figure 18(b)–(d).

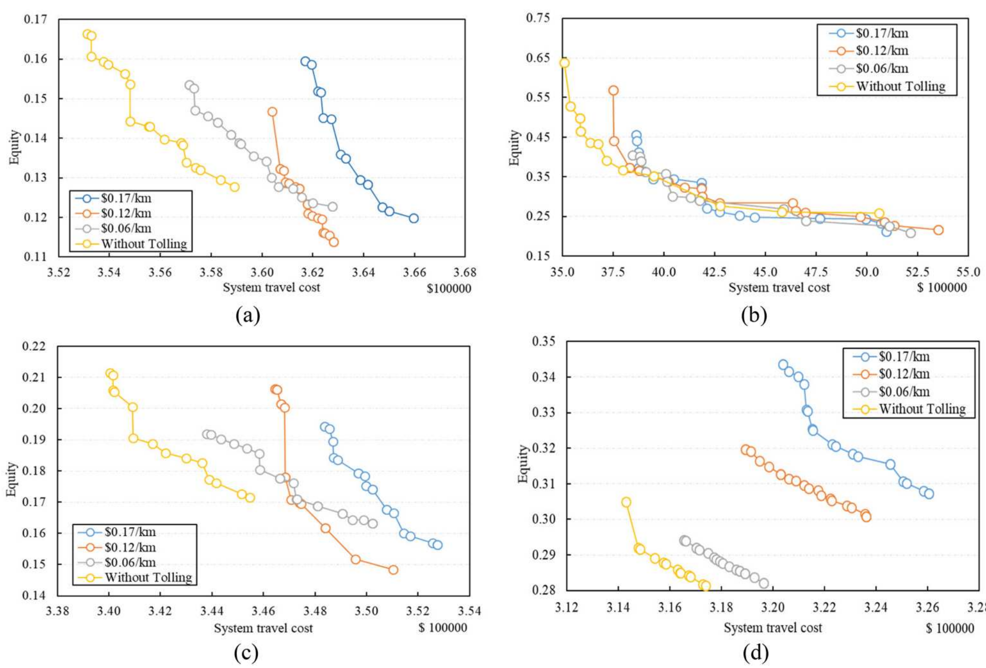

Figure 18. Pareto frontiers with different CAV lane use fees: (a) base scenario, (b) four times base demand, (c) 80% base CAV price, and (d) CAV traveler VOT = $0.2/min.

While it is natural to expect the system travel cost to increase as CAV travelers need to pay for using dedicated CAV lanes, it is more difficult to say about the use fee effect on equity. For the base scenario, imposing a CAV lane use fee of $0.06/km will slightly push the frontier downward. Further increasing the fee to $0.12/km leads to a continued downward movement of the frontier, while the maximum system travel cost on the frontier does not seem to increase. This may be the result of lane and route changes by CAV travelers, by shifting away from dedicated CAV lanes. If the dedicated CAV lane use fee increases to $0.17/km, both equity and system travel cost will get worse, possibly as a result of further lane/route adjustment of CAV travelers.

When travel demand is high (four times the base demand), meaning the network is very congested, the use fee has limited impact on the shape and location of the frontier. When CAV price is dropped to 80% of the base price, the changing trend of Pareto frontier is similar to the base scenario. However, there is an important difference that the frontier with a $0.12/km use fee no longer moves downward compared to the frontier with a $0.06/km use fee. Rather, the frontier covers a wider range of equity values. When CAV traveler VOT is at $0.2/min, imposing and increasing the dedicated CAV lane use fee will exacerbate both system travel cost and equity. This is different from the case of subsidy (where more subsidy improves system travel cost and equity, as shown in Figure 17(c)), and may be attributed to the shift of CAVs away from dedicated CAV lanes to HV lanes, making HV travelers and the whole system worse off.

5.1.4.2. Lane-access restriction strategy. Lane-access restriction strategy means that all CAVs travel exclusively on CAV lanes when such lanes are present on a link. This approach enables the analysis of lane allocation effects on equity. The resulting Pareto frontiers, along with the Pareto frontier without restriction, are shown in Figure 19(a). Further, we also investigate the Pareto frontiers with the strategy under three alternative scenarios: four times base demand, 80% base CAV price, and CAV traveler VOT at $0.2/min. The resulting Pareto frontiers (along with the Pareto frontier without restriction) are displayed in Figure 19(b)–(d).

Figure 19(a) shows that the implementation of the lane-access restriction strategy has mixed effects on system performance and equity. Overall, the strategy results in slight improvements in system travel costs and significant increases in equity, particularly in a lower system travel cost interval. At a system travel cost of about 3.55, the strategy achieves better equity and slightly optimized travel costs. Under high-demand conditions (Figure 19(b)), the strategy significantly exacerbates equity disparities, while the system without lane-access restriction performs better in maintaining equity and shows little difference in travel costs. Base on Figure 19(c), reducing CAV prices by 20% lowers the overall system travel cost and moderately improves the system equity with a restricted strategy. However, equity disparities persist in a lower system travel cost interval. Similarly, a decrease in CAV VOT reduces both CAVs travel costs and the overall system travel cost (Figure 19(d)). At a system travel cost of approximately 3.16, the restriction strategy's impact diverges. Below this threshold, the restriction strategy fails to enhance equity, but above it, equity improves significantly, accompanied by optimized travel costs.

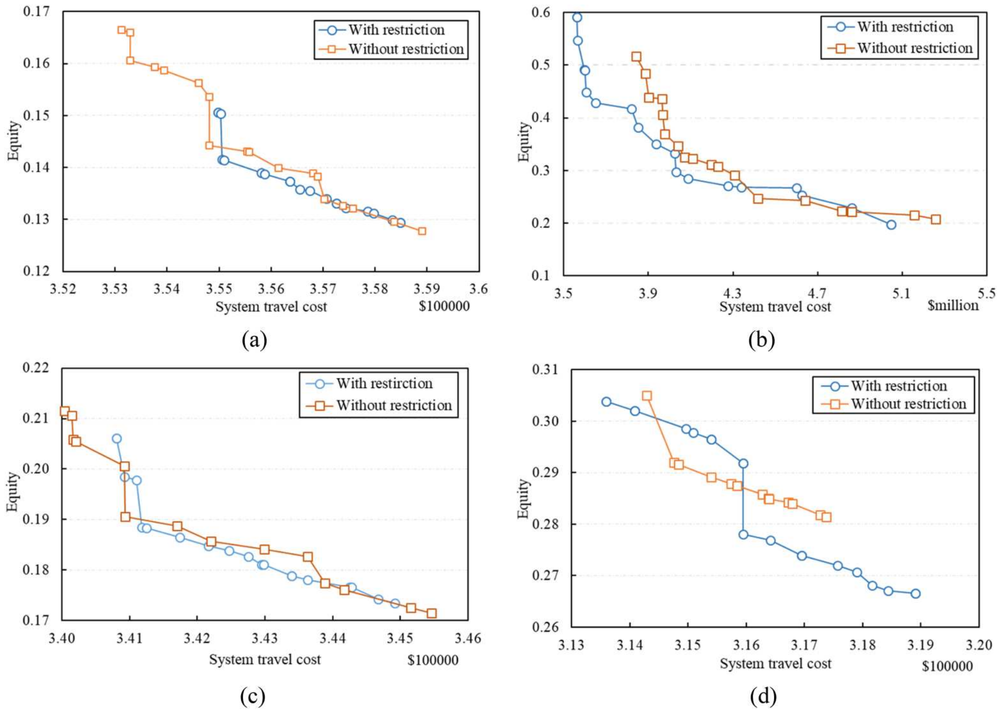

Figure 19. Pareto frontiers with lane-access restriction strategy: (a) base scenario, (b) four times base demand, (c) 80% base CAV price, and (d) CAV traveler VOT = $0.2/min.

These results suggest that while the lane-access restriction strategy can improve system performance and equity in certain contexts, its effectiveness is highly dependent on demand levels, pricing adjustments, and specific system cost invest, and it may inadvertently worsen equity under unfavorable conditions.

5.2. Experiments on south Florida network

In this subsection, we experiment with deploying dedicated CAV lanes on a larger network, the south Florida network (Figure 20). The network consists of 232 physical links, 82 nodes, and 83 OD pairs. In Figure 20, the links with a convertible lane are marked in red. The travel demand on each OD pair is presented in Table 6. Other network data are drawn from Chen et al. (2016). The main modeling parameters remain the same as those for the Nguyen-Dupuis network (Table 3).

Figure 21 shows the resulting Pareto frontier. We observe that the frontier is smoother than the frontier for the Nguyen-Dupuis network (Figure 9). The median value for the equity metric is similar between the two networks (around 0.14). However, the equity value is less sensitive to system travel cost: if we take the two ending points of the frontier, the equity elasticity with respect to system travel cost is only −12.1, much smaller (in absolute value) than the elasticity of the Nguyen-Dupuis network (−246). The equity value range is also narrower, about 0.003 as opposed to 0.04 for the Nguyen-Dupuis network.

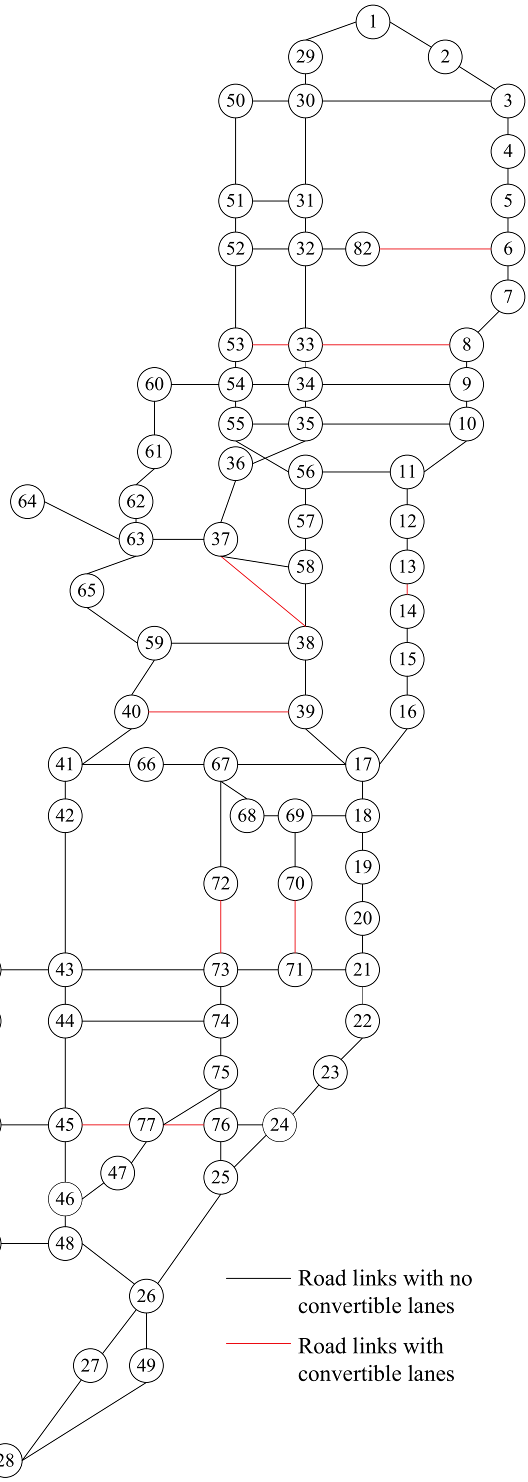

Figure 20. The south Florida network considered.

Table 6. OD demand of the south Florida network.

OD	Demand	OD	Demand	OD	Demand	OD	Demand
1–36	743.56	28–57	743.56	50–19	793.76	64–30	815.3
1–57	860.8	28–63	863.41	50–59	758.15	66–31	768.05
4–64	810.61	29–37	794.11	50–69	806.96	68–5	801.23
5–40	837.18	29–62	806.96	51–21	804.53	70–82	802.1
5–41	862.89	31–70	770.49	51–23	760.76	74–8	826.94
6–42	823.64	32–24	763.02	52–44	768.92	74–33	843.44
7–72	809.91	32–76	848.65	52–71	757.29	75–33	832.32
8–47	847.6	32–80	824.16	53–24	820.68	76–8	777.95
9–46	847.08	33–74	752.6	53–46	798.97	76–33	842.74
10–45	825.72	34–48	812.35	53–75	766.84	76–53	816.17
12–28	810.09	36–1	845.87	54–45	835.45	78–35	828.85
13–2	823.98	40–30	789.77	54–78	841.53	78–53	769.79
14–1	854.38	41–51	846.91	55–48	765.62	78–55	759.89
19–4	843.26	43–7	802.79	55–79	862.37	81–8	767.19
19–50	856.46	44–82	864.97	57–1	832.84	81–33	845
21–51	861.33	45–54	803.49	58–29	774.83	81–52	826.07
24–53	786.64	46–53	745.82	60–1	836.84	82–22	763.89
24–82	797.93	48–8	812	61–1	746.69	82–42	838.4
26–9	825.72	48–55	768.75	61–27	782.3	82–74	811.3
26–10	781.78	49–10	749.82	61–49	815.12	82–80	766.67
28–56	839.27	49–34	865.49	63–29	776.22		

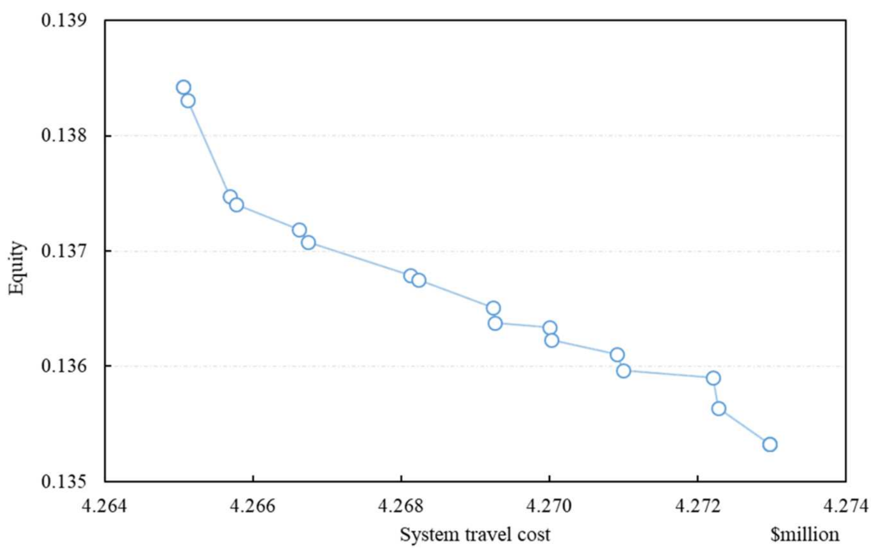

Figure 21. Pareto frontier for the south Florida network.

Figure 22 plots the μ values for each of the 83 ODs and for CAV and HV travelers. While the μ values vary both between CAV and HV travelers of the same OD pair and across different OD pairs, the variations are small overall. In fact, the μ values of a given OD pair between CAV and HV travelers are very similar for most OD pairs, as compared to μ values between different OD pairs. This is consistent with what we observe for the base case of the Nguyen-Dupuis network.

As in Section 5.1.3, we explore the possibility of providing subsidy for HV travelers to improve equity between HV and CAV travelers. The same three levels of subsidy are

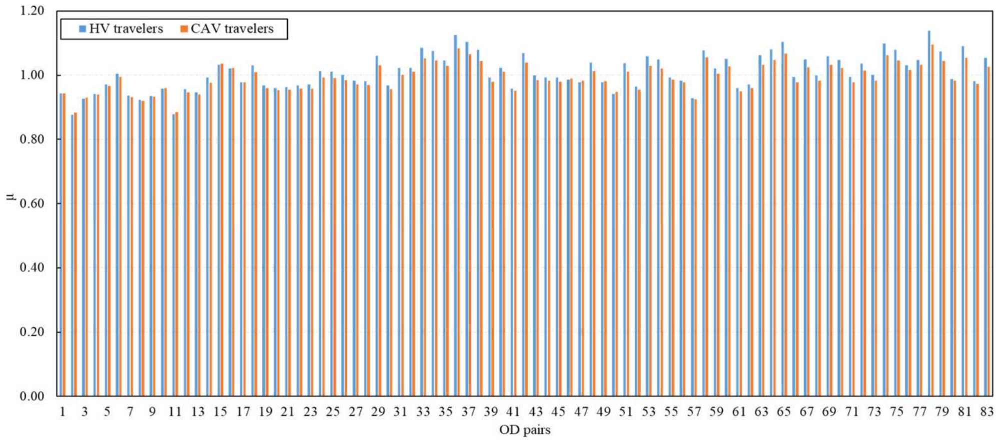

Figure 22. The μ values for CAV and HV travelers on different OD pairs for the south Florida network.

examined: \$0.05/km, \$0.12/km, and \$0.16/km. The resulting frontiers are shown in Figure 23. Unlike the Nguyen-Dupuis network where a small subsidy (\$0.05/km) improves equity, providing subsidy for HV travelers does not improve equity in the south Florida network. In fact, the changing trend is the reverse: more subsidy leads to worse system equity. The reason is that subsidy makes HV travelers much better off than CAV travelers, thereby widening the equity gap and putting CAV travelers in more disadvantageous positions. This can be seen in Figure 24: with a subsidy level of \$0.16/km, the μ values for HV travelers are consistently and noticeably lower than for CAV travelers. On the other hand, subsidizing HV travelers reduces system travel cost. This reduction is always greater than the amount of subsidy provided, as shown in Table 7. Thus, subsidy is justifiable based on economic return, though not from an equity improvement perspective.

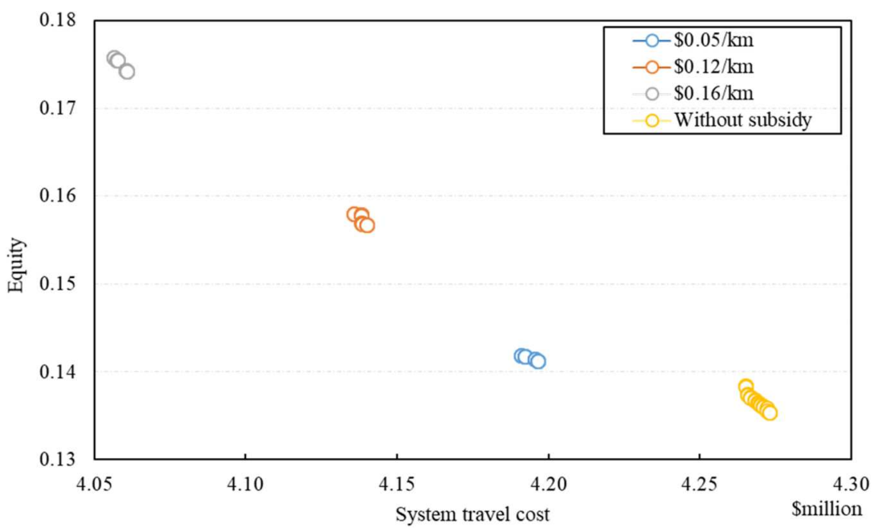

Figure 23. Pareto frontiers with HV traveler subsidy for the south Florida network.

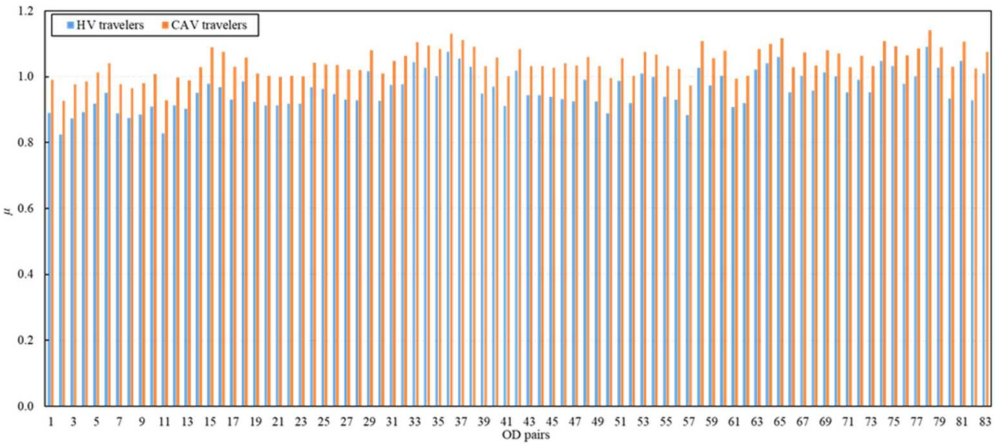

Figure 24. The μ values for CAV and HV travelers on different OD pairs with a subsidy of \$0.16/km for HV travelers, for the south Florida network.

Table 7. Total subsidy, system travel cost reduction, and the ratio of the two under different subsidy levels for the south Florida network.

Subsidy level	Total subsidy (I) (\$)	System travel cost reduction (II) (\$)	Ratio (II/I)
\$0.05/km	58,515	73,918	1.26
\$0.12/km	140,534	129,214	1.01
\$0.16/km	187,835	208,656	1.11

6. Conclusions

The development of CAVs has been gaining significant momentum in recent years. To accommodate CAVs in a mixed traffic environment, this paper investigates the problem of optimally converting some HV lanes to lanes for dedicated CAV use. While this problem has drawn prior research interest, the uniqueness of our study is that we focus on preserving equity, which is important as CAV travelers are likely to benefit from using dedicated CAV lanes while HV travelers may be worse off due to reduced usable road space. To measure equity, a novel metric is proposed based on the value of μ, which is defined as the ratio of travel cost per unit OD distance over the system average μ value, for each OD pair-vehicle type combination. The equity is then measured as the maximum deviation of any μ values from its mean. Minimizing this maximum deviation is sought jointly with minimizing system travel cost through a bi-level bi-objective program, where the decisions are on selecting and converting HV lanes to dedicated CAV lanes. To solve this program, a customized algorithm leveraging the complementary strengths of non-dominated sorting genetic algorithm II and variable neighborhood search is developed.

The bi-level bi-objective program is numerically implemented on a modified Nguyen-Dupuis network and a larger network representing south Florida, yielding a number of findings and insights. Among them, the most interesting findings are: (1) when travel demand is low, equity is not a significant concern. As demand increases, inequity starts to appear, first across different OD pairs and then between CAV and HV travelers.

The latter form of inequity arises because CAV travelers, by taking advantage of the dedicated CAV lanes, are less affected by congestion than HV travelers; (2) as CAVs benefit from lower price and greater automation, the generalized travel cost of CAV travelers will decrease, putting HV travelers at more disadvantageous positions and widening the equity gap. Thus, the need to preserve equity will increase as CAV continues to develop and mature; (3) an adequate amount of subsidy can be effective in mitigating inequity. Subsidy is especially useful when CAV price and CAV traveler VOT are low. Compared to subsidy, introducing a fee for using CAV lanes or lane-access restriction strategy is less promising; (4) the potential use of subsidy is further justified from an economic return perspective, given that the travel cost reduction almost always exceeds the amount of subsidy provided.

For future research, we suggest a few directions. First, the demand side specification could be refined. In the paper, we intend to focus on the short-term effect of CAV lane deployment by assuming fixed travel demand. Further research could treat travel demand to be elastic. Second, the CAV lane deployment may be considered over a planning horizon. Doing so would substantially expand the decision space and time complexity of solving the problem, warranting additional algorithmic examination. Third, other equity metrics employed in the transportation network design literature can be tested, which will help further understand the uniqueness of the equity metric proposed in this study.

Acknowledgement

The financial support of NSF is gratefully acknowledged. The authors also thank the anonymous reviewers for their insightful and constructive comments, which helped us further strengthen the paper.

Disclosure statement

No potential conflict of interest was reported by the author(s).

Funding

The work presented in this paper was supported in part by the US National Science Foundation (NSF) under grant numbers 2112650 and 2330565.

References

Behbahani, H., S. Nazari, M. Jafari Kang, and T. Litman. 2019. “A Conceptual Framework to Formulate Transportation Network Design Problem Considering Social Equity Criteria.” *Transportation Research Part A: Policy and Practice* 125:171–183. https://doi.org/10.1016/j.tra.2018.04.005.

Behbahani, H., S. Nazari, H. Partovifar, and M. J. Kang. 2019. “Designing a Road Network Using John Rawls’s Social Justice Approach.” *Journal of Urban Planning and Development* 145 (2): 05019002. https://doi.org/10.1061/(ASCE)UP.1943-5444.0000500.

Ben-Elia, E., and I. Benenson. 2019. “A Spatially-Explicit Method for Analyzing the Equity of Transit Commuters’ Accessibility.” *Transportation Research Part A: Policy and Practice* 120:31–42. https://doi.org/10.1016/j.tra.2018.11.017.

Bureau of Public Roads. 1964. “Traffic Assignment Manual.” Department of commerce, Urban Planning Division, Washington D.C, U.S.
Chen, D., S. Ahn, M. Chitturi, and D. A. Noyce. 2017. “Towards Vehicle Automation: Roadway Capacity Formulation for Traffic Mixed with Regular and Automated Vehicles.” *Transportation Research Part B: Methodological* 100:196–221. https://doi.org/10.1016/j.trb.2017.01.017.
Chen, Z., F. He, L. Zhang, and Y. Yin. 2016. “Optimal Deployment of Autonomous Vehicle Lanes with Endogenous Market Penetration.” *Transportation Research Part C: Emerging Technologies* 72:143–156. https://doi.org/10.1016/j.trc.2016.09.013.
Chen, A., J. Kim, S. Lee, and Y. Kim. 2010. “Stochastic Multi-Objective Models for Network Design Problem.” *Expert Systems with Applications* 37 (2): 1608–1619. https://doi.org/10.1016/j.eswa.2009.06.048.
Chen, S., H. Wang, and Q. Meng. 2019. “Designing Autonomous Vehicle Incentive Program with Uncertain Vehicle Purchase Price.” *Transportation Research Part C: Emerging Technologies* 103:226–245. https://doi.org/10.1016/j.trc.2019.04.013.
Chen, S., H. Wang, L. Xiao, and Q. Meng. 2022. “Random Capacity for a Single Lane with Mixed Autonomous and Human-Driven Vehicles: Bounds, Mean Gaps and Probability Distributions.” *Transportation Research Part E: Logistics and Transportation Review* 160:102650. https://doi.org/10.1016/j.tre.2022.102650.
Chen, A., and X. Xu. 2012. “Goal Programming Approach to Solving Network Design Problem with Multiple Objectives and Demand Uncertainty.” *Expert Systems with Applications* 39 (4): 4160–4170. https://doi.org/10.1016/j.eswa.2011.09.118.
Deb, K., A. Pratap, S. Agarwal, and T. Meyarivan. 2002. “A Fast and Elitist Multiobjective Genetic Algorithm: NSGA-II.” *IEEE Transactions on Evolutionary Computation* 6 (2): 182–197. https://doi.org/10.1109/4235.996017.
Do, W., O. M. Rouhani, and L. Miranda-Moreno. 2019. “Simulation-based Connected and Automated Vehicle Models on Highway Sections: A Literature Review.” *Journal of Advanced Transportation* 2019:1–14. https://doi.org/10.1155/2019/9343705.
Dworkin, R. 2018. “What is Equality? Part 2: Equality of Resources.” In *The Notion of Equality*, edited by Mane Hajdin, 143–205. London: Routledge.
Farahani, R. Z., E. Miandoabchi, W. Y. Szeto, and H. Rashidi. 2013. “A Review of Urban Transportation Network Design Problems.” *European Journal of Operational Research* 229 (2): 281–302. https://doi.org/10.1016/j.ejor.2013.01.001.
Feng, T., and J. Zhang. 2014. “Multicriteria Evaluation on Accessibility-Based Transportation Equity in Road Network Design Problem.” *Journal of Advanced Transportation* 48 (6): 526–541. https://doi.org/10.1002/atr.1202.
Ferguson, E. M., J. Duthie, and S. T. Waller. 2012. “Comparing Delay Minimization and Emissions Minimization in the Network Design Problem.” *Computer-Aided Civil and Infrastructure Engineering* 27 (4): 288–302. https://doi.org/10.1111/j.1467-8667.2011.00746.x.
Frank, M., and P. Wolfe. 1956. “An Algorithm for Quadratic Programming.” *Naval Research Logistics Quarterly* 3 (1-2): 95–110. https://doi.org/10.1002/nav.3800030109.
Gong, S., J. Shen, and L. Du. 2016. “Constrained Optimization and Distributed Computation Based car Following Control of a Connected and Autonomous Vehicle Platoon.” *Transportation Research Part B: Methodological* 94:314–334. https://doi.org/10.1016/j.trb.2016.09.016.
Greer, L., J. L. Fraser, D. Hicks, M. Mercer, and K. Thompson. 2018. “Intelligent Transportation Systems Benefits, Costs, and Lessons Learned: 2018 Update Report (No. FHWA-JPO-18-641). United States.” Department of Transportation. ITS Joint Program Office.
Guo, Y., M. Hu, B. Zou, M. Hansen, Y. Zhang, and H. Xie. 2022. “Air Traffic Flow Management Integrating Separation Management and Ground Holding: An Efficiency-Equity bi-Objective Perspective.” *Transportation Research Part B: Methodological* 155:394–423. https://doi.org/10.1016/j.trb.2021.12.004.

Hamdan, A., S. Hamdan, M. H. Benbitour, and S. Jradi. 2024. “On the Fair Scheduling of Truck Drivers in Delivery Companies: Balancing Fairness and Profit.” *Central European Journal of Operations Research* 1–26. https://doi.org/10.1007/s10100-023-00899-5.

Han, X., R. Ma, and H. M. Zhang. 2020. “Energy-aware Trajectory Optimization of CAV Platoons Through a Signalized Intersection.” *Transportation Research Part C: Emerging Technologies* 118:102652. https://doi.org/10.1016/j.trc.2020.102652.

Hansen, P., N. Mladenović, and J. A. Moreno Pérez. 2010. “Variable Neighbourhood Search: Methods and Applications.” *Annals of Operations Research* 175 (1): 367–407. https://doi.org/10.1007/s10479-009-0657-6.

Kalra, N., and S. M. Paddock. 2016. “Driving to Safety: How Many Miles of Driving Would it Take to Demonstrate Autonomous Vehicle Reliability?” *Transportation Research Part A: Policy and Practice* 94:182–193. https://doi.org/10.1016/j.tra.2016.09.010.

Kockelman, K., S. Boyles, P. Stone, D. Fagnant, R. Patel, M. W. Levin, G. Sharon, et al. 2017. “An Assessment of Autonomous Vehicles: Traffic Impacts and Infrastructure Needs (No. FHWA/TX-17/0-6847-1).” University of Texas at Austin. Center for Transportation Research.

Kumar, A., S. Guhathakurta, and S. Venkatachalam. 2020. “When and Where Should There be Dedicated Lanes Under Mixed Traffic of Automated and Human-Driven Vehicles for System-Level Benefits?” *Research in Transportation Business & Managemen* 36:100527.

Levin, M. W., and S. D. Boyles. 2016. “A Multiclass Cell Transmission Model for Shared Human and Autonomous Vehicle Roads.” *Transportation Research Part C: Emerging Technologies* 62:103–116.

Li, Y., Z. Chen, Y. Yin, and S. Peeta. 2020. “Deployment of Roadside Units to Overcome Connectivity Gap in Transportation Networks with Mixed Traffic.” *Transportation Research Part C: Emerging Technologies* 111:496–512. https://doi.org/10.1016/j.trc.2020.01.001.

Li, Z., L. Elefteriadou, and S. Ranka. 2014. “Signal Control Optimization for Automated Vehicles at Isolated Signalized Intersections.” *Transportation Research Part C: Emerging Technologies* 49:1–18. https://doi.org/10.1016/j.trc.2014.10.001.

Lin, D.-Y., and C. Xie. 2011. “The Pareto-Optimal Solution set of the Equilibrium Network Design Problem with Multiple Commensurate Objectives.” *Networks and Spatial Economics* 11 (4): 727–751. https://doi.org/10.1007/s11067-010-9146-3.

Litman, T. 2002. *Evaluating Transportation Equity*. Victoria, British Columbia: Victoria Transport Policy Institute.

Litman, T. 2020. *Evaluating Transportation Equity*. Victoria, British Columbia: Victoria Transport Policy Institute.

Liu, J., and A. J. Khattak. 2016. “Delivering Improved Alerts, Warnings, and Control Assistance Using Basic Safety Messages Transmitted Between Connected Vehicles.” *Transportation Research Part C: Emerging Technologies* 68:83–100. https://doi.org/10.1016/j.trc.2016.03.009.

Liu, Z., and Z. Song. 2019. “Strategic Planning of Dedicated Autonomous Vehicle Lanes and Autonomous Vehicle/Toll Lanes in Transportation Networks.” *Transportation Research Part C: Emerging Technologies* 106:381–403. https://doi.org/10.1016/j.trc.2019.07.022.

Lu, Q., T. Tettamanti, D. Hörcher, and I. Varga. 2020. “The Impact of Autonomous Vehicles on Urban Traffic Network Capacity: An Experimental Analysis by Microscopic Traffic Simulation.” *Transportation Letters* 12: 540–549.

Marsh, M. T., and D. A. Schilling. 1994. “Equity Measurement in Facility Location Analysis: A Review and Framework.” *European Journal of Operational Research* 74 (1): 1–17. https://doi.org/10.1016/0377-2217(94)90200-3.

Meng, Q., and H. Yang. 2002. “Benefit Distribution and Equity in Road Network Design.” *Transportation Research Part B: Methodological* 36 (1): 19–35. https://doi.org/10.1016/S0191-2615(00)00036-9.

Miandoabchi, E., F. Daneshzand, W. Y. Szeto, and R. Zanjirani Farahani. 2013. “Multi-objective Discrete Urban Road Network Design.” *Computers & Operations Research* 40 (10): 2429–2449. https://doi.org/10.1016/j.cor.2013.03.016.

Milanés, V., and S. E. Shladover. 2014. "Modeling Cooperative and Autonomous Adaptive Cruise Control Dynamic Responses Using Experimental Data." *Transportation Research Part C: Emerging Technologies* 48:285–300. https://doi.org/10.1016/j.trc.2014.09.001.

Mladenović, N., and P. Hansen. 1997. "Variable Neighborhood Search." *Computers & Operations Research* 24 (11): 1097–1100. https://doi.org/10.1016/S0305-0548(97)00031-2.

Mohammadi, M., P. Jula, and R. Tavakkoli-Moghaddam. 2019. "Reliable Single-Allocation Hub Location Problem with Disruptions." *Transportation Research Part E: Logistics and Transportation Review* 123:90–120. https://doi.org/10.1016/j.tre.2019.01.008.

Noruzoliaee, M., B. Zou, and Y. Liu. 2018. "Roads in Transition: Integrated Modeling of a Manufacturer-Traveler-Infrastructure System in a Mixed Autonomous/Human Driving Environment." *Transportation Research Part C: Emerging Technologies* 90:307–333. https://doi.org/10.1016/j.trc.2018.03.014.

Ogryczak, W. 2000. "Inequality Measures and Equitable Approaches to Location Problems." *European Journal of Operational Research* 122 (2): 374–391. https://doi.org/10.1016/S0377-2217(99)00240-4.

Olivier, P., A. Lodi, and G. Pesant. 2022. "Measures of Balance in Combinatorial Optimization." *4OR* 20 (3): 391–415. https://doi.org/10.1007/s10288-021-00486-x.

Pereira, R. H. M., T. Schwanen, and D. Banister. 2017. "Distributive Justice and Equity in Transportation." *Transport Reviews* 37 (2): 170–191. https://doi.org/10.1080/01441647.2016.1257660.

Pourgholamali, M., M. Miralinaghi, and P. Ha. 2023. "Sustainable Deployment of Autonomous Vehicles Dedicated Lanes in Urban Traffic Networks." *Sustainable Cities and Society* 99:104969. https://doi.org/10.1016/j.scs.2023.104969.

Qu, R. 2018. Mechanism Design for Fair Allocation on Uniform Machines. PhD thesis, University of Warwick.

Rawls, J. 1971. *A Theory of Justice*. Cambridge, MA: Harvard University Press.

Razmi Rad, S., H. Farah, H. Taale, B. van Arem, and S. P. Hoogendoorn. 2020. "Design and Operation of Dedicated Lanes for Connected and Automated Vehicles on Motorways: A Conceptual Framework and Research Agenda." *Transportation Research Part C: Emerging Technologies* 117:102664. https://doi.org/10.1016/j.trc.2020.102664.

Santos, B., A. Antunes, and E. J. Miller. 2008. "Integrating Equity Objectives in a Road Network Design Model." *Transportation Research Record: Journal of the Transportation Research Board* 2089 (1): 35–42. https://doi.org/10.3141/2089-05.

Seilabi, S. E., M. Pourgholamali, G. H. de Almeida Correia, and S. Labi. 2023. "Robust Design of CAV-Dedicated Lanes Considering CAV Demand Uncertainty and Lane Reallocation Policy." *Transportation Research Part D: Transport and Environment* 121:103827. https://doi.org/10.1016/j.trd.2023.103827.

Sharma, S., and T. V. Mathew. 2011. "Multiobjective Network Design for Emission and Travel-Time Trade-off for a Sustainable Large Urban Transportation Network." *Environment and Planning B: Planning and Design* 38 (3): 520–538. https://doi.org/10.1068/b37018.

Shi, F. 2021. "Research on Accessibility and Equity of Urban Transport Based on Multisource big Data." *Journal of Advanced Transportation* 2021:1–18. https://doi.org/10.1155/2021/1103331.

Shladover, S. E. 2018. "Connected and Automated Vehicle Systems: Introduction and Overview." *Journal of Intelligent Transportation Systems* 22 (3): 190–200. https://doi.org/10.1080/15472450.2017.1336053.

Smith, S., J. Bellone, S. Bransfield, A. Ingles, G. Noel, E. Reed, and M. Yanagisawa. 2015. "Benefits Estimation Framework for Automated Vehicle Operations (No. FHWA-JPO-16-229; DOT-VNTSC-FHWA-15-12)." United States. Departmant of Transportation. ITS Joint Program Office.

Sohn, K. 2011. "Multi-objective Optimization of a Road Diet Network Design." *Transportation Research Part A: Policy and Practice* 45 (6): 499–511. https://doi.org/10.1016/j.tra.2011.03.005.

Sumalee, A., S. Shepherd, and A. May. 2009. "Road User Charging Design: Dealing with Multi-Objectives and Constraints." *Transp* 36:167–186.

Szeto, W. Y., and H. K. Lo. 2006. “Transportation Network Improvement and Tolling Strategies: The Issue of Intergeneration Equity.” *Transportation Research Part A: Policy and Practice* 40 (3): 227–243. https://doi.org/10.1016/j.tra.2005.06.004.

Talebian, A., and S. Mishra. 2022. “Unfolding the State of the Adoption of Connected Autonomous Trucks by the Commercial Fleet Owner Industry.” *Transportation Research Part E: Logistics and Transportation Review* 158: 102616.

Talebpour, A., and H. S. Mahmassani. 2016. “Influence of Connected and Autonomous Vehicles on Traffic Flow Stability and Throughput.” *Transportation Research Part C: Emerging Technologies* 71:143–163. https://doi.org/10.1016/j.trc.2016.07.007.

Tientrakool, P., Y.-C. Ho, and N. F. Maxemchuk. 2011. “Highway Capacity Benefits from Using Vehicle-to-Vehicle Communication and Sensors for Collision Avoidance.” In *2011 IEEE Vehicular Technology Conference (VTC Fall)*, 1–5. San Francisco, CA: IEEE.

Vahidi, A., and A. Sciarretta. 2018. “Energy Saving Potentials of Connected and Automated Vehicles.” *Transportation Research Part C: Emerging Technologies* 95:822–843. https://doi.org/10.1016/j.trc.2018.09.001.

van den Berg, V. A. C., and E. T. Verhoef. 2016. “Autonomous Cars and Dynamic Bottleneck Congestion: The Effects on Capacity, Value of Time and Preference Heterogeneity.” *Transportation Research Part B: Methodological* 94:43–60. https://doi.org/10.1016/j.trb.2016.08.018.

Wang, J., L. Lu, S. Peeta, and Z. He. 2021. “Optimal Toll Design Problems Under Mixed Traffic Flow of Human-Driven Vehicles and Connected and Autonomous Vehicles.” *Transportation Research Part C: Emerging Technologies* 125:102952. https://doi.org/10.1016/j.trc.2020.102952.

Wang, Y., and W. Y. Szeto. 2017. “Multiobjective Environmentally Sustainable Road Network Design Using Pareto Optimization: Environmentally Sustainable Road Network Design Using Pareto Optimization.” *Computer-Aided Civil and Infrastructure Engineering* 32 (11): 964–987. https://doi.org/10.1111/mice.12305.

Wardrop, J. G. 1952. “Some Theoretical Aspects of Road Traffic Research.” *Proceedings of the Institution of Civil Engineers - Transport* 1:325–362.

Yang, H., and H.-J. Huang. 2004. “The Multi-Class, Multi-Criteria Traffic Network Equilibrium and Systems Optimum Problem.” *Transportation Research Part B: Methodological* 38 (1): 1–15. https://doi.org/10.1016/S0191-2615(02)00074-7.

Yang, H., and X. Zhang. 2002. “Multiclass Network Toll Design Problem with Social and Spatial Equity Constraints.” *Journal of Transportation Engineering* 128 (5): 420–428. https://doi.org/10.1061/(ASCE)0733-947X(2002)128:5(420).

Ye, Y., and H. Wang. 2018. “Optimal Design of Transportation Networks with Automated Vehicle Links and Congestion Pricing.” *Journal of Advanced Transportation* 2018:1–12. https://doi.org/10.1155/2018/3435720.

Ye, L., and T. Yamamoto. 2018. “Impact of Dedicated Lanes for Connected and Autonomous Vehicle on Traffic Flow Throughput.” *Physica A: Statistical Mechanics and its Applications* 512:588–597. https://doi.org/10.1016/j.physa.2018.08.083.

Yu, B., L. Kong, Y. Sun, B. Yao, and Z. Gao. 2015. “A Bi-Level Programming for bus Lane Network Design.” *Transportation Research Part C: Emerging Technologies* 55:310–327. https://doi.org/10.1016/j.trc.2015.02.014.

Zhu, D., T. Xie, Y. Liu, B. Zou, and N. Rujeerapaiboon. 2023. “Optimal Deployment of an Equitable CAV Platoonable Corridor on Road Networks with Mixed Traffic Flow.” *Transportation Research Part C: Emerging Technologies* 157:104399. https://doi.org/10.1016/j.trc.2023.104399.

Zografos, K. G., and Y. Jiang. 2019. “A Bi-Objective Efficiency-Fairness Model for Scheduling Slots at Congested Airports.” *Transportation Research Part C: Emerging Technologies* 102:336–350. https://doi.org/10.1016/j.trc.2019.01.023.

Appendix

Equivalency between the KKT conditions of the minimization problem in Section 3.3.2 and equilibrium conditions (12) and (20)–(21)

The Lagrangian of the minimization problem of expression (23) subject to (11), (12), (16), and (17) can be written as:

$$L(\boldsymbol{f}_m, \boldsymbol{\lambda}) = Z(\boldsymbol{V}(\boldsymbol{f}_m)) + \sum_{w \in W} \lambda_w^m \left(D_m^w - \sum_{r \in R_w^m} f_{w,m}^r \right) \tag{A1}$$

where λ_w^m is the Lagrange multiplier for vehicle type m of OD pair w. The first-order KKT conditions of the Lagrangian is as follows:

$$f_{w,m}^r \frac{\partial L(\boldsymbol{f}_m, \boldsymbol{\lambda})}{\partial f_{w,m}^r} = 0; \quad \frac{\partial L(\boldsymbol{f}_m, \boldsymbol{\lambda})}{\partial f_{w,m}^r} \geq 0; \quad f_{w,m}^r \geq 0 \qquad \forall\, m \in M, w \in W, \; r \in R_w^m \tag{A2}$$

To investigate the derivatives in the above conditions, let us consider an arbitrary route r of OD pair w:

$$\frac{\partial L(\boldsymbol{f}_m, \boldsymbol{\lambda})}{\partial f_{w,m}^r} = \frac{\partial Z(\boldsymbol{V}(\boldsymbol{f}_m))}{\partial f_{w,m}^r} + \frac{\partial}{\partial f_{w,m}^r} \sum_{w \in W} \lambda_w^m \left(D_m^w - \sum_{r \in R_w^m} f_{w,m}^r \right) \tag{A3}$$

where the first term on the right-hand side can be further derived using chain rule:

$$\frac{\partial Z(\boldsymbol{V}(\boldsymbol{f}_m))}{\partial f_{w,m}^r} = \sum_{\hat{\mathcal{A}}_2} \left[\frac{\partial Z(\boldsymbol{V})}{\partial v_b^{\mathrm{HV}}} \frac{\partial v_b^{\mathrm{HV}}}{f_{w,m}^r} + \frac{\partial Z(\boldsymbol{V})}{\partial v_b^{\mathrm{CAV}}} \frac{\partial v_b^{\mathrm{CAV}}}{f_{w,m}^r} \right] + \sum_{b \in \hat{\mathcal{A}}_1} \frac{\partial Z(\boldsymbol{V})}{\partial v_b^{\mathrm{CAV}}} \frac{\partial v_b^{\mathrm{CAV}}}{f_{w,m}^r} \tag{A4}$$

For $\dfrac{\partial Z(\boldsymbol{V})}{\partial v_b^{\mathrm{HV}}}$, we have:

$$\begin{aligned} \frac{\partial Z(\boldsymbol{V}(\boldsymbol{f}_m))}{\partial v_b^{\mathrm{HV}}} &= \frac{\partial}{\partial v_b^{\mathrm{HV}}} \left[\sum_a \int_0^{v_a} t_a(x) dx + \sum_a \frac{1}{\eta_{\mathrm{HV}}} v_a^{\mathrm{HV}} l_a U_{\mathrm{HV}} \right] \\ &= \frac{\partial \int_0^{v_b} t_b(x) dx}{\partial v_b} \frac{\partial v_b}{\partial v_b^{\mathrm{HV}}} + \frac{1}{\eta_{\mathrm{HV}}} l_b U_{\mathrm{HV}} \\ &= t_b(v_b) + \frac{1}{\eta_{\mathrm{HV}}} l_b U_{\mathrm{HV}}. \end{aligned} \tag{A5}$$

where $U_{\mathrm{HV}} = \dfrac{\kappa_{\mathrm{HV},1} \kappa_{\mathrm{HV},2}}{\kappa_{\mathrm{HV},3} \kappa_{\mathrm{HV},4} \kappa_{\mathrm{HV},5}} \rho_{\mathrm{HV}} + \dfrac{VC_{\mathrm{HV}}}{\kappa_{\mathrm{HV},5}}$. . The last equality is because $v_b = v_b^{\mathrm{HV}} + v_b^{\mathrm{CAV}}$. Thus, $\dfrac{\partial v_b}{\partial v_b^{\mathrm{HV}}} = \dfrac{\partial v_b^{\mathrm{HV}}}{\partial v_b^{\mathrm{HV}}} + \dfrac{\partial v_b^{\mathrm{CAV}}}{\partial v_b^{\mathrm{HV}}} = 1 + 0 = 1.$

For $\dfrac{\partial Z(\boldsymbol{V})}{\partial v_b^{\mathrm{CAV}}}$, we can similarly derive the following, with U_{CAV} defined the same as U_{HV} except changing the subscript:

$$\frac{\partial Z(\boldsymbol{V})}{\partial v_b^{\mathrm{CAV}}} = t_b(v_b) + \frac{1}{\eta_{\mathrm{CAV}}} l_b U_{\mathrm{CAV}} \tag{A6}$$

We further note that $\frac{\partial v_b^{\mathrm{HV}}}{\partial f_{w,\mathrm{HV}}^r} = \delta_{b,r}^{\mathrm{HV},w}$, $\frac{\partial v_b^{\mathrm{CAV}}}{\partial f_{w,\mathrm{CAV}}^r} = \delta_{b,r}^{\mathrm{CAV},w}$, $\frac{\partial v_b^{\mathrm{HV}}}{\partial f_{w,\mathrm{CAV}}^r} = 0$, and $\frac{\partial v_b^{\mathrm{CAV}}}{\partial f_{w,\mathrm{HV}}^r} = 0$, we have:

$$\frac{\partial Z[\boldsymbol{V}(\boldsymbol{f}_m)]}{\partial f_{w,m}^r} = \begin{cases} \sum\limits_{b\in\bar{\mathcal{A}}\cup\hat{\mathcal{A}}_2}\left[t_b(v_b) + \frac{1}{\eta_{\mathrm{HV}}} l_b U_{\mathrm{CAV}}\right]\delta_{b,r}^{\mathrm{HV},w} = \frac{c_{w,\mathrm{HV}}^r}{\eta_{\mathrm{HV}}} & \text{if } m = \mathrm{HV} \\ \sum\limits_{b\in\mathcal{A}}\left[t_b(v_b) + \frac{1}{\eta_{\mathrm{CAV}}} l_b U_{\mathrm{CAV}}\right]\delta_{b,r}^{\mathrm{CAV},w} = \frac{c_{w,\mathrm{CAV}}^r}{\eta_{\mathrm{HV}}} & \text{if } m = \mathrm{CAV} \end{cases} \tag{A7}$$

For the second term of Equation (A3), we have:

$$\frac{\partial}{\partial f_{w,m}^r}\sum_{w\in W}\lambda_w^m\left(D_m^w - \sum_{r\in R_w^m} f_{w,m}^r\right) = \frac{\partial}{\partial f_{w,m}^r}\sum_{w\in W}\lambda_w^m D_m^w - \frac{\partial}{\partial f_{w,m}^r}\sum_{w\in W}\lambda_w^m\sum_{r\in R_w^m} f_{w,m}^r \tag{A8}$$

where the first term on the right-hand side is zero. Thus we only need to look at the second term. Because $\frac{\partial f_{w,m}^r}{\partial f_{w,m}^r} = \begin{cases} 1, & w = w \text{ and } r = r \\ 0, & \text{otherwise} \end{cases}$, we have:

$$\frac{\partial}{\partial f_{w,m}^r}\sum_{w\in W}\lambda_w^m\left(D_m^w - \sum_{r\in R_w^m} f_{w,m}^r\right) = -\lambda_w^m \tag{A9}$$

With the above derivations, the first-order KKT conditions (A2) can be written as:

$$f_{w,m}^r(c_{w,m}^r - \eta_m\lambda_w^m) = 0 \quad \forall\, m \in M, w \in W,\ r \in R_w^m \tag{A10}$$

$$c_{w,m}^r - \eta_m\lambda_w^m \geq 0 \quad \forall\, m \in M, w \in W,\ r \in R_w^m \tag{A11}$$

$$f_{w,m}^r \geq 0 \quad \forall\, m \in M, w \in W,\ r \in R_w^m \tag{A12}$$

With $\eta_m\lambda_w^m = C_w^m$, (A10)-(A12) is the same as equilibrium conditions (12) and (20)–(21).